Two multilayered plate models with transverse shear warping functions issued from three dimensional elasticity equations

Alexandre Loredo, Alexis Castel

Two multilayered plate models with transverse shear warping functions issued from three dimensional elasticity equations

A. Loredo[a,*], A. Castel[a]

[a] *DRIVE, Université de Bourgogne, 49 rue Mlle Bourgeois, 58027 Nevers, France*

Abstract

A multilayered plate theory which uses transverse shear warping functions issued from three-dimensional elasticity is presented. Two methods to obtain these transverse shear warping functions are detailed. The warping functions are issued from the variations of transverse shear stresses computed at special location points for a simply supported bending problem. The first method considers an exact 3D solution of the problem. The second method uses the solution provided by the model itself: the transverse shear stresses are computed by the integration of equilibrium equations. Hence, an iterative process is applied, the model being updated with the new warping functions, and so on. These two models are compared to other models and to analytical solutions for the bending of simply supported plates. Four different laminates and a sandwich are considered, length-to-thickness values varying from 2 to 100. An additional analytical solution that simulates the behavior of laminates under the plane stress hypothesis – which is retained by all presented models – shows that the iterative model almost gives the exact solution for all laminates and all length-to-thickness ratio values.

Keywords: Plate theory, warping function, laminate, multilayered, composite, sandwich, vibration

1. Introduction

In many human-built structures, plates and shells are present. These particular structures are distinguished from others because a dimension – the transverse dimension – is much smaller than the others. Hence, although it is always possible, their representation through a three-dimensional domain is not the better way to study them. To understand and forecast their mechanical behavior, plate models have been developed. These models permit to study plates and shells through a two-dimensional domain while allowing at least membrane and bending deformations. What happens in the third direction is not ignored, it is precisely the purpose of the plate model to integrate the transverse behavior into its equations. The more precise this behavior is integrated, the more accurate the model will behave. History starts with early works of Kirchhoff, Love, and Rayleigh [1–3] leading to the Love-Kirchhoff model in which no shear deformation is allowed. Because of the limitation of this model to thin plates, authors like Reissner, Uflyand, and Mindlin[4–6] have proposed to integrate a shear deformation of order 1 in z leading to the Mindlin-Reissner model. These two aforementioned models were proposed for homogeneous plates but their pendent for laminated structures have been later proposed and are actually called the Classical Lamination Theory (CLT) and the First-order Shear Deformation Theory (FSDT). The last one has been improved by the use of shear correction factors [7–9]. The need to improve this accuracy have been motivated by the study of thick plates and laminated plates. In both cases, the early plate models fail to give precise results. It is even worse if some layers have small mechanical properties compared to others, which is the case for sandwich structures or when viscoelastic layers are used to improve the damping. To overcome these difficulties, specific models have been proposed. However, a universal model that can manage plates of various length-to-thickness ratios, with any lamination scheme and various materials including functionally graded materials, with good accuracy for the static, dynamic, and damped dynamic behaviors is still a challenge.

Dealing with multilayered plates have given rise to another class of theories, called the Layer-Wise (LW) models, in which the number of unknowns depend on the number of layers, by opposition to the Equivalent

*Corresponding author
Email addresses: alexandre.loredo@u-bourgogne.fr (A. Loredo), alexis.castel@u-bourgogne.fr (A. Castel)

Single Layer (ESL) family of models in which the number of unknown is independent of the number of layers. Obviously, LW models are expected to be more precise than ESL models but they are less easy to use for complex structures and require more computational resources than ESL models. This has motivated searchers to propose ESL models in which the transverse shear is taken into account in a more precise way than for the first models. Following the classification given by Carrerra [10], we can see two approaches that have given interesting models:

- First, the Vlasov-Reddy [11] theory, also called Higher Shear Deformation Theory (HSDT), later followed by other higher order theories, proposes kinematic fields with a third-order dependence on z, motivated by the respect of the nullity of transverse shear at top and bottom faces of the plate. Other functions (trigonometric, hyperbolic...) have been proposed by other authors [12–14] to integrate the transverse shear in the kinematic field . Note that these models do not integrate informations about the lamination sequence in their kinematic field, and do not verify the transverse stress continuity at interfaces.

- Second, some *a priori* LW models can reduce to ESL models with the help of assumptions between the fields in each layer. Zig-Zag (ZZ) models enter in this category. Early works of Lekhnitskii [15] and Ambartsumyan [16] have been classified as such by Carrera [10] who shows also that other authors have integrated the multilayer structure in their model [17–19] in a very similar manner. The main idea of ZZ models is to let in-plane displacements vary with z according to the superposition of a zig-zag law to a global law – cubic for example. With these models, shear stresses can satisfy both continuity at interfaces and null (or prescribed) values at top and bottom faces of the plate.

In the last category, more recent works can be cited like Refs. [9, 20, 21] and the reader may also refer to recent reviews on the subject [22, 23].

In this work, the kinematic assumptions are similar of those taken in Ref. [21] but they differ because no precise choice of the functions describing the transverse behavior is done. These functions, called *warping functions* (WF) are the core of the model. The model has been entirely formulated in [24] and it has been shown that, according to specific choices of the WF, it can also represent most of the classical models (CLT, FSDT, HSDT) and others, as it will appear in the following. However, and it is precisely the subject of this article, is is possible to choose and adapt the WF in a completely free manner.

This article presents two different ways of obtaining new sets of WF issued from three dimensional elasticity laws. The first way consists to build the WF from three-dimensional solutions. Three-dimensional solutions for the bending of laminates have been obtained since early works of [25, 26] and have been recently obtained for general lamination schemes [27]. These solutions are obtained for particular boundary conditions and load, which can be seen as the principal limitation of their use in the present model. The second way is to derive the WF from the equilibrium equations. This lead to an iterative model: starting with "classical" WF, for example Reddy's formula, WF are issued from the equilibrium equations and then integrated to the model, and so on until that no significant change is detected on the WF. This second method could be of practical interest because it might be used locally, for example at Gauss' points in Finite Element, in order to build a local model which will be sensitive to the local material sequence and to the local deformation state, including the dynamic behavior if needed.

2. Considered plate theory

In this section, we recall the main components of the theory presented in Ref. [24]. It is a plate theory based on the use of transverse shear WF. It allows the simulation of multilayer laminates made of orthotropic plies using different sets of transverse shear WF. The purpose of this paper is to propose enhanced WF issued from 3D elasticity equations (see section 3), but several plate models (among ESL and ZZ models) issued from the literature can also be formulated in terms of transverse shear WF, as it was shown in Ref. [24]. This is of practical interest when comparing results issued from different models, because these models can be implemented in a similar manner.

2.1. Laminate definition and index convention

The laminate, of height h, is composed of N layers. All the quantities will be related to those of the middle plane[1] which is placed at $z = 0$; they are marked with the superscript 0. In the following, Greek subscripts takes values 1 or 2 and Latin subscripts takes values 1, 2 or 3. The Einstein's summation convention is used for subscripts only. The comma used as a subscript index means the partial derivative with respect to the following(s) index(ices).

2.2. Displacement field

The kinematic assumptions of the theory are:

$$\begin{cases} u_\alpha(x,y,z) &= u^0_\alpha(x,y) - z w^0_{,\alpha}(x,y) + \varphi_{\alpha\beta}(z)\gamma^0_{\beta 3}(x,y) \\ u_3(x,y,z) &= w^0(x,y) \end{cases} \tag{1}$$

where $u^0_\alpha(x,y)$, $w^0(x,y)$ and $\gamma^0_{\alpha 3}(x,y)$, are respectively the in-plane displacements, the deflection and the engineering transverse shear strains evaluated at the middle plane. The $\varphi_{\alpha\beta}(z)$ are the four WF. The associated strain field is derived from equation (1):

$$\begin{cases} \varepsilon_{\alpha\beta}(x,y,z) = \varepsilon^0_{\alpha\beta}(x,y) - z w^0_{,\alpha\beta}(x,y) + \frac{1}{2}\left(\varphi_{\alpha\gamma}(z)\gamma^0_{\gamma 3,\beta}(x,y) + \varphi_{\beta\gamma}(z)\gamma^0_{\gamma 3,\alpha}(x,y)\right) & \text{(2a)} \\ \varepsilon_{\alpha 3}(x,y,z) = \frac{1}{2}\varphi'_{\alpha\beta}(z)\gamma^0_{\beta 3}(x,y) & \text{(2b)} \\ \varepsilon_{33}(x,y,z) = 0 & \text{(2c)} \end{cases}$$

which, with the use of Hooke's law, leads to the following stress field:

$$\begin{cases} \sigma_{\alpha\beta}(x,y,z) = Q_{\alpha\beta\gamma\delta}(z)\left(\varepsilon^0_{\gamma\delta}(x,y) - z w^0_{,\gamma\delta}(x,y) + \varphi_{\gamma\mu}(z)\gamma^0_{\mu 3,\delta}(x,y)\right) & \text{(3a)} \\ \sigma_{\alpha 3}(x,y,z) = C_{\alpha 3\beta 3}(z)\varphi'_{\beta\mu}(z)\gamma^0_{\mu 3}(x,y) & \text{(3b)} \\ \sigma_{33}(x,y,z) = 0 & \text{(3c)} \end{cases}$$

where $Q_{\alpha\beta\gamma\delta}(z)$ are the generalized plane stress stiffnesses and $C_{\alpha 3\beta 3}(z)$ are the components of Hooke's tensor corresponding to the transverse shear stiffnesses.

2.3. Static laminate behavior

The model requires introduction of generalized forces:

$$\begin{cases} \{N_{\alpha\beta}, M_{\alpha\beta}, P_{\gamma\beta}\} = \displaystyle\int_{-h/2}^{h/2} \{1, z, \varphi_{\alpha\gamma}(z)\}\sigma_{\alpha\beta}(z)\mathrm{d}z & \text{(4a)} \\ Q_\beta = \displaystyle\int_{-h/2}^{h/2} \varphi'_{\alpha\beta}(z)\sigma_{\alpha 3}(z)\mathrm{d}z & \text{(4b)} \end{cases}$$

They are then set, by type, into vectors:

$$\mathbf{N} = \begin{Bmatrix} N_{11} \\ N_{22} \\ N_{12} \end{Bmatrix} \quad \mathbf{M} = \begin{Bmatrix} M_{11} \\ M_{22} \\ M_{12} \end{Bmatrix} \quad \mathbf{P} = \begin{Bmatrix} P_{11} \\ P_{22} \\ P_{12} \\ P_{21} \end{Bmatrix} \quad \mathbf{Q} = \begin{Bmatrix} Q_1 \\ Q_2 \end{Bmatrix} \tag{5}$$

and the same is done for the corresponding generalized strains:

$$\boldsymbol{\epsilon} = \begin{Bmatrix} \epsilon^0_{11} \\ \epsilon^0_{22} \\ 2\epsilon^0_{12} \end{Bmatrix} \quad \boldsymbol{\kappa} = \begin{Bmatrix} -w^0_{,11} \\ -w^0_{,22} \\ -2w^0_{,12} \end{Bmatrix} \quad \boldsymbol{\Gamma} = \begin{Bmatrix} \gamma^0_{13,1} \\ \gamma^0_{23,2} \\ \gamma^0_{13,2} \\ \gamma^0_{23,1} \end{Bmatrix} \quad \boldsymbol{\gamma} = \begin{Bmatrix} \gamma^0_{13} \\ \gamma^0_{23} \end{Bmatrix} \tag{6}$$

[1] The reference plane can be arbitrarily chosen in the laminate assuming that the corresponding transverse shear WF are adapted in consequence.

Generalized forces are linked with the generalized strains by the 10×10 and 2×2 following stiffness matrices:

$$\begin{Bmatrix} \mathbf{N} \\ \mathbf{M} \\ \mathbf{P} \end{Bmatrix} = \begin{bmatrix} \mathbf{A} & \mathbf{B} & \mathbf{E} \\ \mathbf{B} & \mathbf{D} & \mathbf{F} \\ \mathbf{E^T} & \mathbf{F^T} & \mathbf{G} \end{bmatrix} \begin{Bmatrix} \boldsymbol{\epsilon} \\ \boldsymbol{\kappa} \\ \boldsymbol{\Gamma} \end{Bmatrix} \quad \{\mathbf{Q}\} = [\mathbf{H}] \{\boldsymbol{\gamma}\} \tag{7}$$

with the following definitions:

$$\begin{cases} \{A_{\alpha\beta\gamma\delta}, B_{\alpha\beta\gamma\delta}, D_{\alpha\beta\gamma\delta}, E_{\alpha\beta\mu\delta}, F_{\alpha\beta\mu\delta}, G_{\nu\beta\mu\delta}\} = \displaystyle\int_{-h/2}^{h/2} Q_{\alpha\beta\gamma\delta}(z)\{1, z, z^2, \varphi_{\gamma\mu}(z), z\varphi_{\gamma\mu}(z), \varphi_{\alpha\nu}(z)\varphi_{\gamma\mu}(z)\}\mathrm{d}z \\ H_{\alpha 3\beta 3} = \displaystyle\int_{-h/2}^{h/2} \varphi'_{\gamma\alpha}(z) C_{\gamma 3\delta 3}(z) \varphi'_{\delta\beta}(z)\mathrm{d}z \end{cases} \tag{8a}$$

(8b)

2.4. Laminate equations of motion

Weighted integration of equilibrium equations leads to

$$\begin{cases} N_{\alpha\beta,\beta} = R\ddot{u}^0_\alpha - S\ddot{w}^0_{,\alpha} + U_{\alpha\beta}\ddot{\gamma}^0_{\beta 3} & \text{(9a)} \\ M_{\alpha\beta,\beta\alpha} + q = R\ddot{w}^0 + S\ddot{u}^0_{\alpha,\alpha} - T\ddot{w}^0_{,\alpha\alpha} + V_{\alpha\beta}\ddot{\gamma}^0_{\beta 3,\alpha} & \text{(9b)} \\ P_{\alpha\beta,\beta} - Q_\alpha = U_{\beta\alpha}\ddot{u}^0_\beta - V_{\beta\alpha}\ddot{w}^0_{,\beta} + W_{\alpha\beta}\ddot{\gamma}^0_{\beta 3} & \text{(9c)} \end{cases}$$

where $q = [\sigma_{33}(z)]^{h/2}_{-h/2}$ is the value of the transverse loading (no tangential forces are applied on the top and bottom of the plate), and:

$$\{R, S, T, U_{\alpha\beta}, V_{\alpha\beta}, W_{\alpha\beta}\} = \int_{-h/2}^{h/2} \rho(z)\{1, z, z^2, \varphi_{\alpha\beta}(z), \varphi_{\alpha\beta}(z)z, \varphi_{\mu\alpha}(z)\varphi_{\mu\beta}(z)\}\mathrm{d}z \tag{10}$$

3. Warping functions issued from transverse shear stress analysis

We introduce two different ways to obtain WF from transverse shear stress analysis: a first set of WF is issued from an analytical solution and a second set is issued from an iterative process using the integration of equilibrium equations. We shall examine first a way to link the searched WF to given shear stresses.

3.1. From transverse shear stresses to WF

Considering equation (3b), we see that the $\varphi'_{\alpha\beta}$ are directly linked to the $\sigma_{\alpha 3}$. Introducing the transverse shear stresses $\sigma^0_{\delta 3}(x, y)$ at $z = 0$ into this equation lead to

$$\sigma_{\alpha 3}(x, y, z) = 4C_{\alpha 3\beta 3}(z)\varphi'_{\beta\gamma}(z)S_{\gamma 3\delta 3}(0)\sigma^0_{\delta 3}(x, y) \tag{11}$$

where $S_{\gamma 3\delta 3}$ are components of the compliance tensor.

This can be written

$$\sigma_{\alpha 3}(x, y, z) = \Psi'_{\alpha\beta}(z)\sigma^0_{\beta 3}(x, y) \tag{12}$$

where:

$$\Psi'_{\alpha\beta}(z) = 4C_{\alpha 3\delta 3}(z)\varphi'_{\delta\gamma}(z)S_{\gamma 3\beta 3}(0) \tag{13}$$

The $\Psi'_{\alpha\beta}(z)$ cannot be issued directly from equation (12) because there are four functions to determine from two stresses leading to infinitely many solutions. The main idea is to consider a simply supported plate submitted to a bi-sine load, and to make the four functions $\Psi'_{\alpha\beta}(z)$ fit the transverse shear stresses in two separate locations

on the plate. Since the deformation of the plate is of the form (19), the transverse shear stresses at the reference plane are of the form:

$$\begin{cases} \sigma^0_{13}(x,y) = s_{13}\cos(\xi x)\sin(\eta y) + \overline{s}_{13}\sin(\xi x)\cos(\eta y) & \text{(14a)} \\ \sigma^0_{23}(x,y) = s_{23}\sin(\xi x)\cos(\eta y) + \overline{s}_{23}\cos(\xi x)\sin(\eta y) & \text{(14b)} \end{cases}$$

These shear stresses are evaluated at specific points A and B for which:

- at point A, $x = a/2$ and $y = 0$, then $\sigma^0_{13}(A) = \overline{s}_{13}$ and $\sigma^0_{23}(A) = s_{23}$
- at point B, $x = 0$ and $y = b/2$, then $\sigma^0_{13}(B) = s_{13}$ and $\sigma^0_{23}(B) = \overline{s}_{23}$

Setting these local values into formula (12) leads to the following system:

$$\begin{bmatrix} s_{13} & 0 & \overline{s}_{23} & 0 \\ 0 & s_{23} & 0 & \overline{s}_{13} \\ \overline{s}_{13} & 0 & s_{23} & 0 \\ 0 & \overline{s}_{23} & 0 & s_{13} \end{bmatrix} \begin{Bmatrix} \Psi'_{11} \\ \Psi'_{22} \\ \Psi'_{12} \\ \Psi'_{21} \end{Bmatrix} = \begin{Bmatrix} \sigma^0_{13}(B) \\ \sigma^0_{23}(A) \\ \sigma^0_{13}(A) \\ \sigma^0_{23}(B) \end{Bmatrix} \tag{15}$$

The $\Psi'_{\alpha\beta}(z)$ are obtained from the resolution of this system; $\varphi'_{\alpha\beta}(z)$ are then obtained using the reciprocal of equation (13):

$$\varphi'_{\alpha\beta}(z) = 4S_{\alpha 3\delta 3}(z)\Psi'_{\delta\gamma}(z)C_{\gamma 3\beta 3}(0) \tag{16}$$

Then, integrating the $\varphi'_{\alpha\beta}(z)$ so that $\varphi_{\alpha\beta}(0) = 0$ gives the four WF $\varphi_{\alpha\beta}(z)$.

3.2. WF issued from exact 3D solutions

Exact 3D solutions of simply supported plates submitted to a bi-sine load are known for cross-ply and antisymmetric angle-ply laminates since the works of Pagano [25] and Noor [28]. Further works have shown that they can be obtained by several ways. Solution for general lamination have been proposed recently in Ref. [27]. The corresponding plate problem is solved with the appropriate method, and the transverse shear stresses are computed at the points A and B. Then, the procedure described in the previous section is applied.

3.3. WF issued from equilibrium equation integration

Since transverse shear stresses can be obtained from equilibrium equation integration, it is also possible to get the warping functions following an iterative process[2]. The process, described in the algorithm 1, starts with any known WF, says Reddy's $z/h - 4/3(z/h)^3$ formula for example, and, at each iteration, the model is updated with WF issued from the transverse stresses of the previous iteration. The procedure is also based on the simply supported plate bending problem with a bi-sine loading. Let us establish the needed formulas, starting from the equilibrium conditions within a solid, without body forces:

$$\begin{cases} \sigma_{\alpha\beta,\beta} + \sigma_{\alpha 3,3} = \rho\ddot{u}_\alpha & \text{(17a)} \\ \sigma_{\alpha 3,\alpha} + \sigma_{33,3} = \rho\ddot{u}_3 & \text{(17b)} \end{cases}$$

The transverse shear stresses, for the static case, are therefore computed using:

$$\begin{aligned} \sigma_{\alpha 3}(z) &= -\int_{-h/2}^{z} \sigma_{\alpha\beta,\beta}(z)\mathrm{d}z \\ &= -\int_{-h/2}^{z} Q_{\alpha\beta\gamma\delta}(z)\left(u^0_{\gamma,\delta\beta}(x,y) - z w^0_{,\gamma\delta\beta}(x,y) + \varphi_{\gamma\mu}(z)\gamma^0_{\mu 3,\delta\beta}(x,y)\right)\mathrm{d}z \end{aligned} \tag{18}$$

Then, the spatial derivatives of the generalized displacements are eliminated accounting to the specific nature of the chosen basis (19).

[2] This iterative process, although based on a simpler formulation, has been proposed in the 1989 unpublished reference [29]

Algorithm 1: Obtaining warping functions from equilibrium equations

Set i=0, $w_0 = 0$;
Take Reddy's formula as WF;
repeat
  i=i+1;
  Compute stiffness matrices;
  Solve the displacements with Navier's method;
  Assign the deflection to w_i;
  Compute transverse shear stresses using equation (18);
  Compute new WF using 3.1;
until $\left|\dfrac{w_i - w_{i-1}}{w_i}\right| >= \epsilon$;

3.4. Discussion

The two ways to obtain WF from transverse shear stresses described in the above sections are based on the study of a simply supported plate submitted to a bi-sine load. As one shall see in the following, the two methods gives very similar results. This proves that the model, which is strongly implicated in the iterative process, is able to fit the transverse shear stresses of the 3D solution with good agreement. Of course, there is no guarantee at this time that these WF will be the best candidates if another plate problem is studied, with different boundary conditions and/or different loading. It is precisely the reason why the iterative process is interesting because it might be adapted to a local strategy.

4. Solving method by a Navier-like procedure

A Navier-like procedure is implemented to solve both static and dynamic problems for a simply supported plate. For the static case, in order to respect the simply supported boundary condition for laminates which are not of cross-ply nor anti-symmetrical angle-ply types, a specific loading is applied using a Lagrange multiplier as it is presented below. The dynamic study is restricted to the search of the natural frequencies.

The Fourier series is limited to one term, hence the generalized displacement field is

$$\begin{Bmatrix} u_1 \\ u_2 \\ w \\ \gamma_{13} \\ \gamma_{23} \end{Bmatrix} = \begin{Bmatrix} u_1^{mn} \cos(\xi x) \sin(\eta y) & +\overline{u}_1^{mn} \sin(\xi x) \cos(\eta y) \\ u_2^{mn} \sin(\xi x) \cos(\eta y) & +\overline{u}_2^{mn} \cos(\xi x) \sin(\eta y) \\ w^{mn} \sin(\xi x) \sin(\eta y) & +\overline{w}^{mn} \cos(\xi x) \cos(\eta y) \\ \gamma_{13}^{mn} \cos(\xi x) \sin(\eta y) & +\overline{\gamma}_{13}^{mn} \sin(\xi x) \cos(\eta y) \\ \gamma_{23}^{mn} \sin(\xi x) \cos(\eta y) & +\overline{\gamma}_{23}^{mn} \cos(\xi x) \sin(\eta y) \end{Bmatrix} \tag{19}$$

with

$$\xi = \frac{m\pi}{a} \text{ and } \eta = \frac{n\pi}{b}$$

where a and b are the length of the sides of the plate, m and n are wavenumbers, set to 1 for static analysis or to arbitrary values for the dynamic study of the corresponding mode. Then for a given m and n, the motion equations of section 2.4 give a stiffness and a mass matrix, respectively $[\mathbf{K}]$ and $[\mathbf{M}]$, related to the vector $\{\mathbf{U}\} = \{u_1^{mn}, u_2^{mn} \ldots \overline{\gamma}_{13}^{mn} \overline{\gamma}_{23}^{mn}\}$. The static case is treated solving the linear system $[\mathbf{K}]\{\mathbf{U}\} = \{\mathbf{F}\}$, where $\{\mathbf{F}\}$ is a force vector containing q^{mn} for its third component (generally set to one). Solving the dynamic case consists in researching the generalized eigenvalues for matrices $[\mathbf{K}]$ and $[\mathbf{M}]$. For cross-ply and antisymmetric angle ply, w respects the simply supported conditions, i. e. $\overline{w}_{mn} = 0$. For the general laminates, the deflection under a bi-sine loading gives a $\overline{w}_{mn} \neq 0$. Since we choose to keep simply supported boundary conditions, $\overline{w}_{mn}$ may be set to zero if a bi-cosine term is added to the loading. The amplitude of the bi-cosine term $\overline{q}^{mn}$ is obtained using a Lagrange multiplier. The stiffness matrix is then of size 11×11.

$$\left[\begin{array}{c|c} \mathbf{K} & \mathbf{C} \\ \hline \mathbf{C}^T & 0 \end{array}\right] \left\{\begin{array}{c} \mathbf{U} \\ \hline \overline{q}_{mn} \end{array}\right\} = \left\{\begin{array}{c} \mathbf{F} \\ \hline 0 \end{array}\right\} \tag{20}$$

with $\{\mathbf{C}\}$ being a vector with on a one on it's eighth component. For the dynamic case, the matrix $[\mathbf{M}]$ is augmented with a line and a column of zeros so it becomes a 11×11 matrix. Detailed formulation of matrices $[\mathbf{K}]$ and $[\mathbf{M}]$ are given in Appendix A.1. Note that it is also possible to keep the loading of the form $q(x, y) = q^{mn} \sin(\xi x) \sin(\eta y)$, then the simply supported boundary condition is no longer respected for general laminates.

5. Numerical results

This section proposes the study of five configurations including four laminates and a sandwich. Only two materials are involved, an orthotropic composite material for all laminates and an honeycomb-type material for the core of the sandwich panel. All the properties are given in table 1.

The results obtained with the models involving WF issued from the two methods described in section 3 are compared to results obtained with different models issued from the literature. As these models can be implemented by means of WF, the solving process described in section 4 can be applied to all models. An exact three dimensional analytical solution is also computed for all test cases. As mentioned before, this solution (denoted Exa in tables) is used to create a WF set as explained in section 3, but it also gives deflections and natural frequencies taken as reference for comparisons.

Another exact solution is computed with stiffness values modified to fit the generalized plane stress assumption. It is done setting $E_3 = 10^{10} E_2$ and $\nu_{13} = \nu_{23} = 0$ for each material. This last solution is of particular interest because, as we shall see later, it shows that the two aforementioned models are very accurate according to the plane stress assumption, and also shows that this assumption is no longer accurate when a/h takes small values. It is designated in tables by the Exa^2 symbol. For all exact solutions, the loading is divided into two equal parts which are applied to the top and bottom faces.

	E_1	E_2	E_3	G_{23}	G_{13}	G_{12}	ν_{23}	ν_{13}	ν_{12}	ρ
Composite ply (p)	$25E_2^p$	10^6	E_2^p	$0.2E_2^p$	$0.5E_2^p$	$0.5E_2^p$	0.25	0.25	0.25	1500
Core material (c)	E_2^c	4×10^4	$12.5E_2^c$	$1.5E_2^c$	$1.5E_2^c$	$1.5E_2^c$	0.25	0.25	0.25	100

Table 1: Material properties

Three nondimensionalized quantities are considered and compared to those issued from analytical solutions:

– Deflections w are nondimensionalized using equation

$$w^* = 100 \frac{E_2^{\text{ref}} h^3}{(-q)a^4} w \tag{21}$$

– First natural frequencies are nondimensionalized using equation

$$\omega^* = \frac{a^2}{h} \sqrt{\frac{\rho^{\text{ref}}}{E_2^{\text{ref}}}} \omega \tag{22}$$

– Shear stresses are nondimensionalized using equation

$$\sigma^*_{\alpha 3} = 10 \frac{h}{(-q)a} \sigma_{\alpha 3} \tag{23}$$

where E_2^{ref} and ρ^{ref} are taken as values of the core material for the sandwich and as values of the composite ply for laminates.

Calculations obtained with WF issued from transverse shear stresses of analytical solutions (denoted 3D in tables) and iterative process (denoted Ite in tables) are compared to those obtained with WF corresponding to classical models that are formulated as follows:

– First order Shear Deformation Theory: this formulation is the Mindlin-Reissner plate theory (denoted MR in tables) which can be formulated setting in the generic model the following warping functions,

$$\varphi_{\alpha\beta}(z) = \delta^K_{\alpha\beta} z \tag{24}$$

where $\delta^K_{\alpha\beta}$ is Kronecker's delta. Note that this theory is generally used with shear correction factors, at least the 5/6 factor which corresponds to an homogeneous plate. As there is several ways to compute them in the general case, we chose in this study not to use them, what is of course a serious penalty for this model.

– High order Shear Deformation Theory: this formulation is Reddy's third order theory (denoted Red in tables), it verifies that transverse shear stresses are null at the top and bottom planes of the plate. It can be emulated by means of the following warping functions:

$$\varphi_{\alpha\beta}(z) = \delta^K_{\alpha\beta}\left(z - \frac{4}{3}\frac{z^3}{h^2}\right) \tag{25}$$

– Sun & Whitney, Woodcock: This model (denoted SW in tables) defines a zig-zag displacement field which verifies the continuity of transverse shear stresses at the layers' interfaces. It was first presented in Ref. [18] and generalized in Ref. [30]. It is also possible to formulate this model with warping functions as shown in [24]:

$$\varphi_{\alpha\beta}(z) = 4C_{\gamma 3\beta 3}(0)\int_{-h/2}^{z} S_{\alpha 3\gamma 3}(\zeta)\mathrm{d}\zeta \tag{26}$$

– Efficient Higher-Order Plate Theory: This formulation, presented by Cho[3] [19, 31] (denoted Cho in tables) consists in superimposing a cubic displacement field, which permits the transverse shear stresses to be null at the top and bottom planes of the laminates, to a zig-zag displacement field issued from the continuity of the transverse shears stresses at the layer interfaces. The corresponding WF, which are polynomials of third order in z, are not detailed. Indeed, as their computation needs the solving of a system of equations, it is difficult to give here an explicit form. Note also that for coupled laminates, an extension of this model [21] has been proposed. This model has not been implemented in this study, it could have given different results for the $[-15/15]$ case which is the only coupled laminate considered in this study.

5.1. Rectangular [0/90/0] cross-ply composite plate

This composite plate is made of three plies with the properties mentioned in table 1 with a [0/90/0] stacking sequence and $b = 3a$. Results are presented in table 2. Note that Reddy's model – with relatively simple WF – gives quite good results for this laminate. Cho's model – with more sophisticated WF – gives better values than the previous, except for the $a/h = 2$ length-to-thickness ratio. Results also show that the two present models, 3D and Ite, give a very satisfying accuracy for all length-to-thickness ratios. Compared to other models with reference to the exact solution, values for the deflection are among the best results, values for the transverse stresses at points A and B, and for the first natural frequency, are the best. However, we can note a weakness for the prediction of $\sigma_{23}(A)$, which is probably due to a sandwich-like behavior of this laminate according to the y direction. The SW model, which is accurate with sandwiches, tends to confirm this point. Both present model, even though warping functions are generated with two very different methods, give almost identical results. Compared to the Exa[2] plane stress exact solution, the model with iterative WF gives the exact solution for this problem. This point will be discussed later on section 5.6.

Figure 1 shows the corresponding WF for $a/h = 4$, for all plate models except the MR. Figure 2 shows transverse shear variation through the thickness obtained by the integration of equilibrium equations for all models, compared to the exact solution, in the $a/h = 4$ case.

[3] In reference [10], Carrera said that this model was a re-discovery of previous works, and called the model the Ambartsumyan-Whitney-Rath-Das theory.

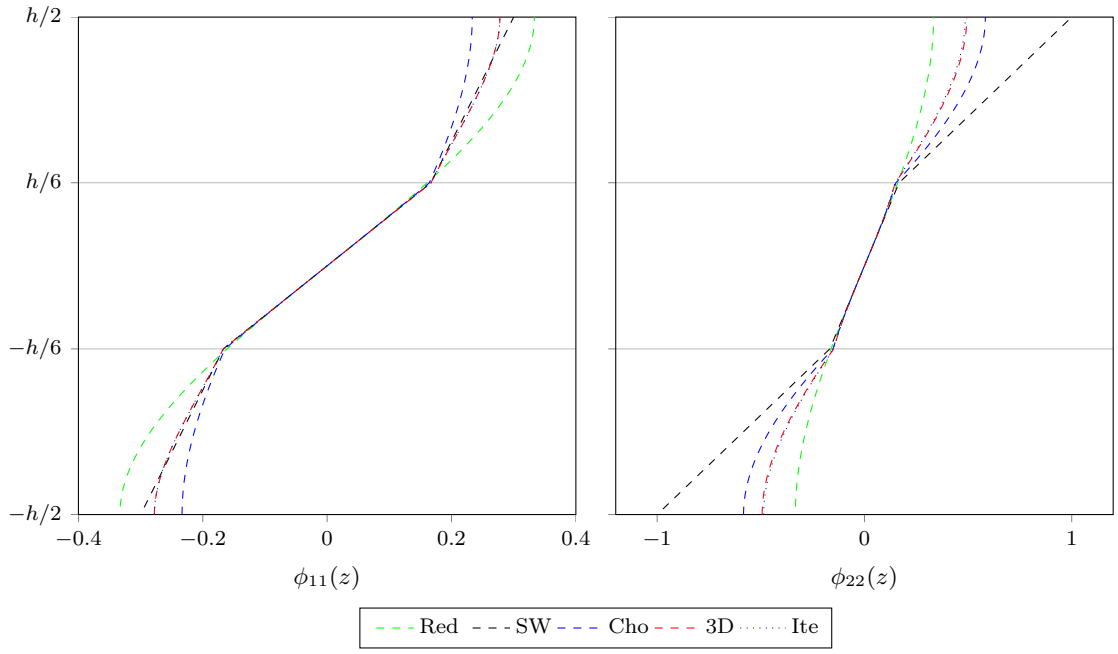

Figure 1: Transverse shear WF of the rectangular [0/90/0] composite plate with $a/h = 4$ for each model.

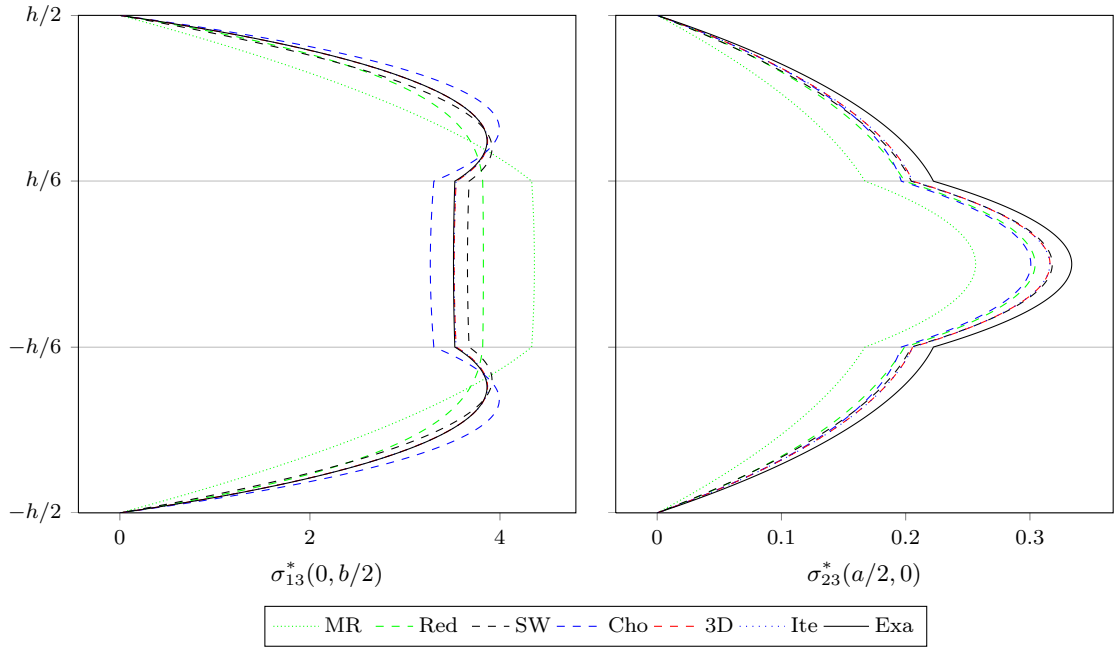

Figure 2: Nondimensionalized transverse shear stresses of the rectangular [0/90/0] composite plate with $a/h = 4$ for each model.

5.2. Square [0/c/0] sandwich plate

In order to study the behavior of a structure exhibiting a high variation of stiffness through the thickness, we propose to study a square sandwich plate with ply thicknesses $h_1 = h_3 = 0.1h$ and $h_2 = 0.8h$. The face sheets are made of one ply of unidirectional composite and the core is constituted of a honeycomb-type material. Material properties are presented in table 1. Results presented in table 3 show this time that Reddy's model is not as good as than for the previous case, although Cho's model obtain better values. This is due to the particular nature of sandwich materials which gives typically zig-zag variations for displacements through the thickness and then typically zig-zag WF. Cho's model is able to fit this kind of variation although Reddy's model is not. The SW model has also been proved to be very efficient for sandwiches, which can be verified in this table. Note that the two present models globally gives the best results. Comparison with the Exa^2 model is discussed in section 5.6.

Figure 3 shows the corresponding WF for $a/h = 4$, for all plate models except the MR. Figure 4 presents the transverse shear stresses at points A and B obtained for all models by the integration of equilibrium equations, compared to the exact solution, in the $a/h = 4$ case.

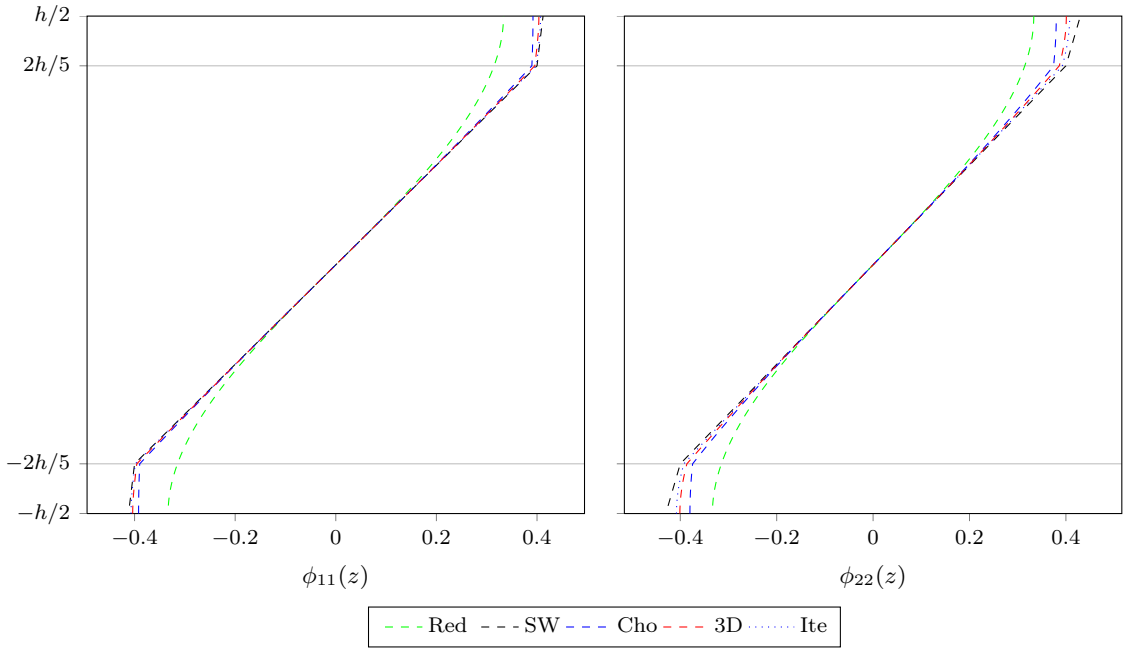

Figure 3: Transverse shear WF of the [0/c/0] sandwich plate with $a/h = 4$ for each model.

5.3. Square [−15/15] antisymmetric angle-ply composite plate

As the two previous cases enters in the cross-ply family, let us now consider an antisymmetric angle-ply square plate with two layers of equal thicknesses and stacking sequence [−15/15]. Transverse stresses $\sigma_{23}(0, b/2, z)$ and $\sigma_{13}(a/2, 0, z)$ are no longer null for this laminate but $\sigma_{23}(B)$ and $\sigma_{13}(A)$ are. Hence, these stresses have been computed respectively at points $D(0, b/2, h/2)$ and $C(a/2, 0, h/2)$ in order to make comparisons between all models. Results are presented in table 4. The tendency of predictions is almost the same than for the [0/90/0] case but it can be noticed that poor values are obtained for the stresses at points D and C. These values are influenced by the way the model is able to couple the x and y direction in the kinematic field, *i.e.* the presence of non null $\varphi_{12}(z)$ and $\varphi_{21}(z)$ functions. This is only the case for the Cho, 3D and Ite models. However, Cho's model does not give very good values for the lowest length-to-thickness values, but it was also the case for the [0/90/0] laminate, which may signify that the problem comes from another reason. The two present models, 3D and Ite, globally gives the best results, but also with quite poor estimations of transverse stresses at points C and D in the $a/h = 2$ case. Comparison with the Exa^2 model is let to the section 5.6.

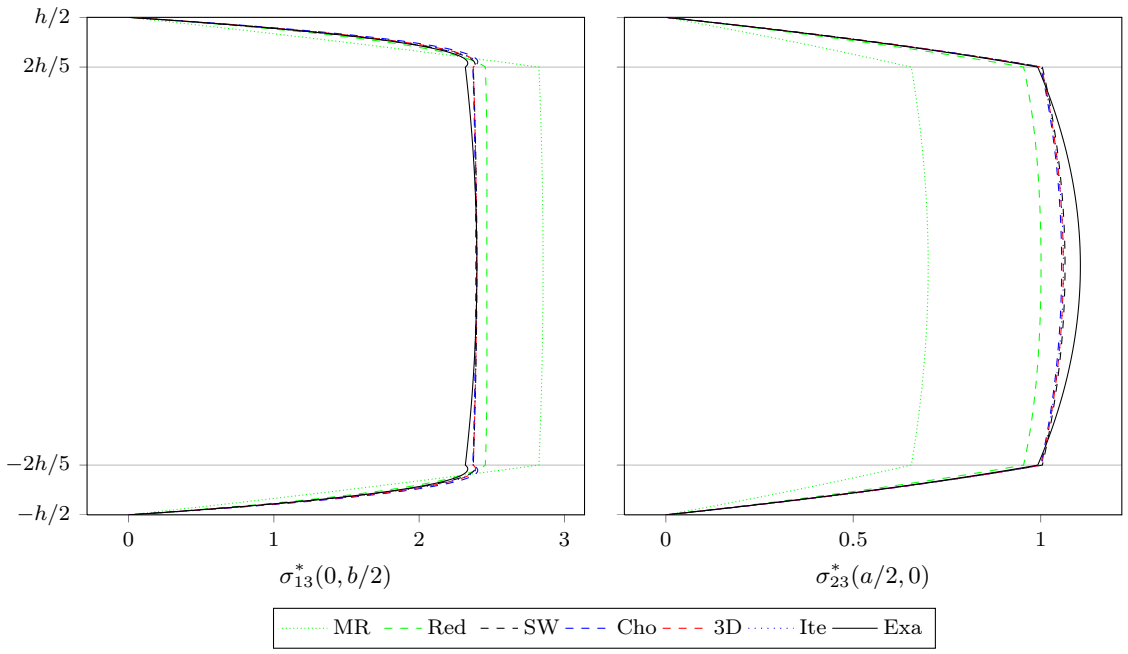

Figure 4: Nondimensionalized transverse shear stresses of the $[0/c/0]$ sandwich plate with $a/h = 4$ for each model.

Figure 5 shows the corresponding WF for $a/h = 4$, for all plate models except the MR. Figure 6 presents the transverse shear stresses at points A and B obtained for all models by the integration of equilibrium equations, compared to the exact solution, in the $a/h = 4$ case.

5.4. Square [0] *single ply composite plate*

This square composite plate is made of a single ply with the properties mentioned in table 1. In this single layer case, the MR model (without shear correction factors) and the SW exactly coincides. It is also the case for Cho's and Reddy's models. Note that the x and y directions are not equivalent for the considered laminate, but even for Cho's model, in this case, $\varphi_{11}(z) = \varphi_{22}(z)$. This is not true for 3D and Ite models which exhibits different $\varphi_{11}(z)$ and $\varphi_{22}(z)$ functions due to the different longitudinal/shear modulus ratios in each direction. Note also that, even if it cannot be seen in the figures presented in this paper, the WF for these two models depend on the length-to-thickness ratio. Present models, 3D and Ite, give poorer values for the deflection than Reddy's model. However, the stresses and the fundamental frequency are best predicted. As we shall see later in section 5.6, the plane stress hypothesis is no longer valid for such low length-to-thickness ratios, that is the reason why the Exa^2 solution has been introduced.

Figure 7 shows the corresponding WF for $a/h = 4$, for all plate models except the MR. Figure 8 presents the transverse shear stresses at points A and B obtained for all models by the integration of equilibrium equations, compared to the exact solution, in the $a/h = 4$ case.

5.5. Square [0/30/0] *composite plate*

Let us now consider a symmetric angle-ply square plate with three layer of equal thicknesses and stacking sequence [0/30/0]. This configuration is chosen since it doesn't involve any simplification in the linear system (20), i. e. matrix $[\mathbf{K}]$ doesn't have any null coefficient. Although this laminate does not represent the more general case (because of its symmetry) it involves an additional $\overline{q}^{mn}\cos(\xi x)\cos(\eta y)$ term in the loading to fulfill the simply supported condition. In other words, it is the only laminate considered in this study which requires a (non-null) Lagrange multiplier in the solving process presented in section 4. Results presented in table 6 show the same tendency than for the [0] laminate, which in fact is not so different. Present models, 3D and Ite, give globally better stresses and fundamental frequency, and a poorer deflection, compared to Reddy's or Cho's model when the Exa solution is taken as reference.

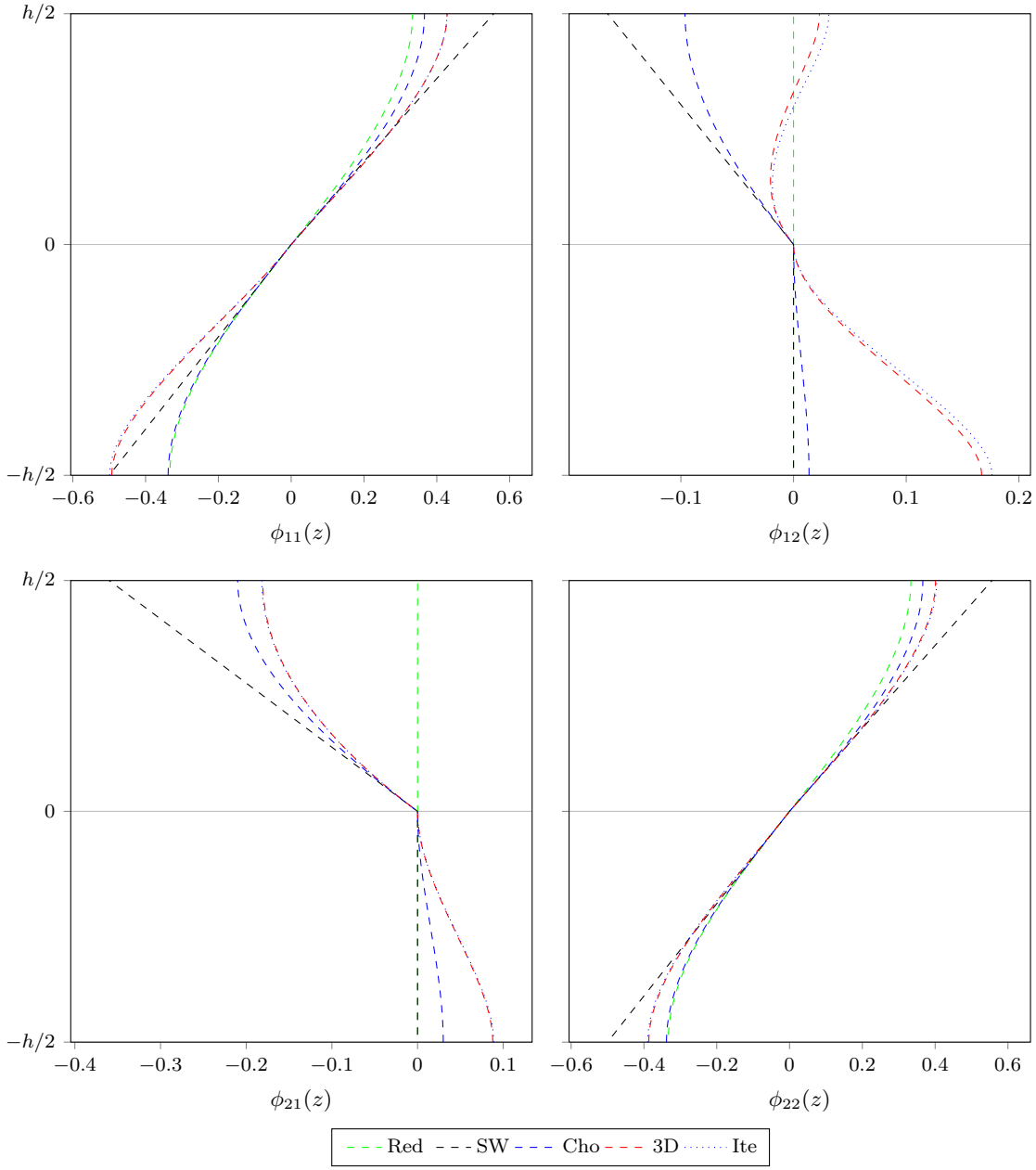

Figure 5: Transverse shear WF of the $[-15/15]$ antisymmetric angle-ply composite plate with $a/h = 4$ for each model.

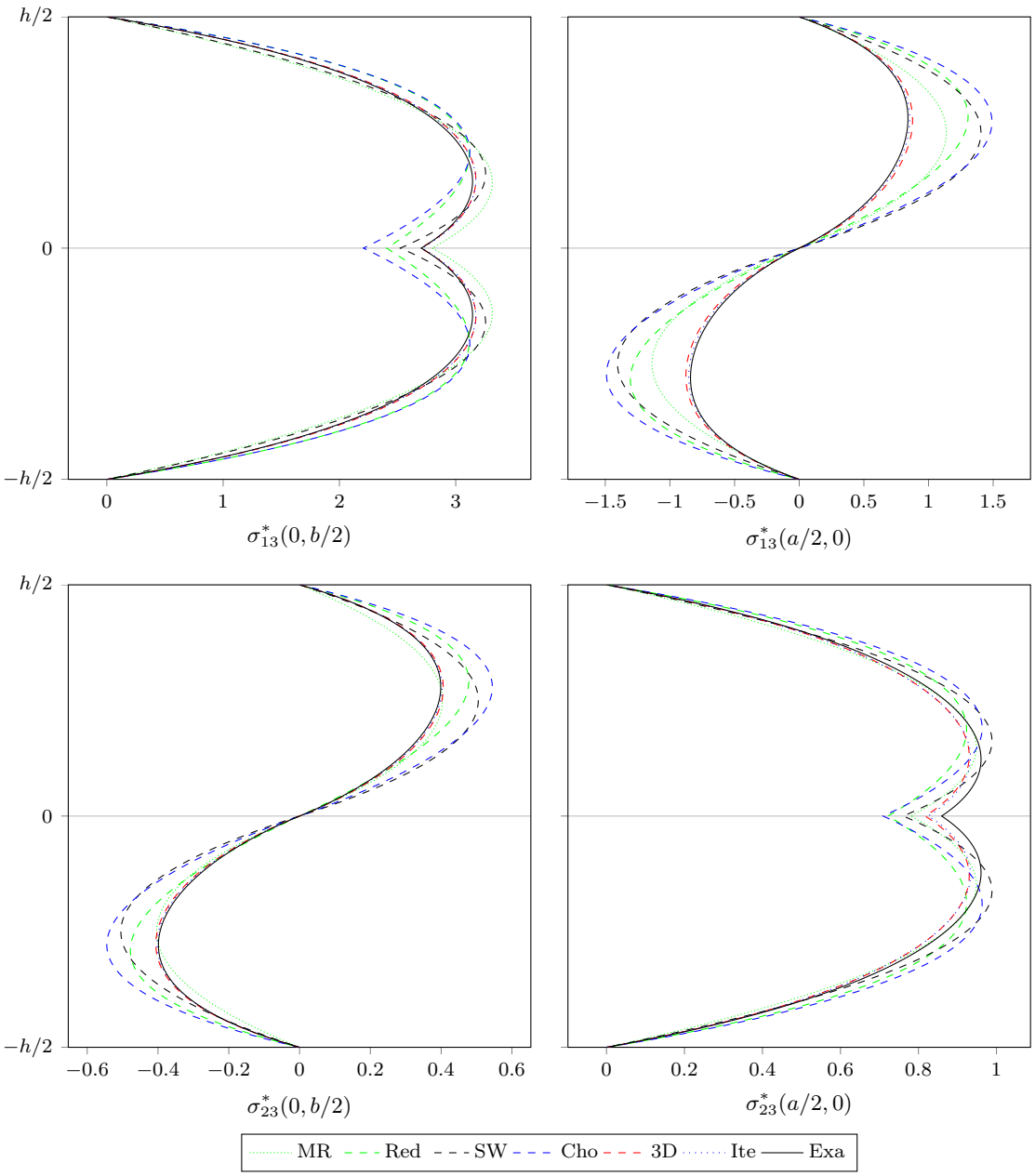

Figure 6: Nondimensionalized transverse shear stresses of the $[-15/15]$ antisymmetric angle-ply composite plate with $a/h = 4$ for each model.

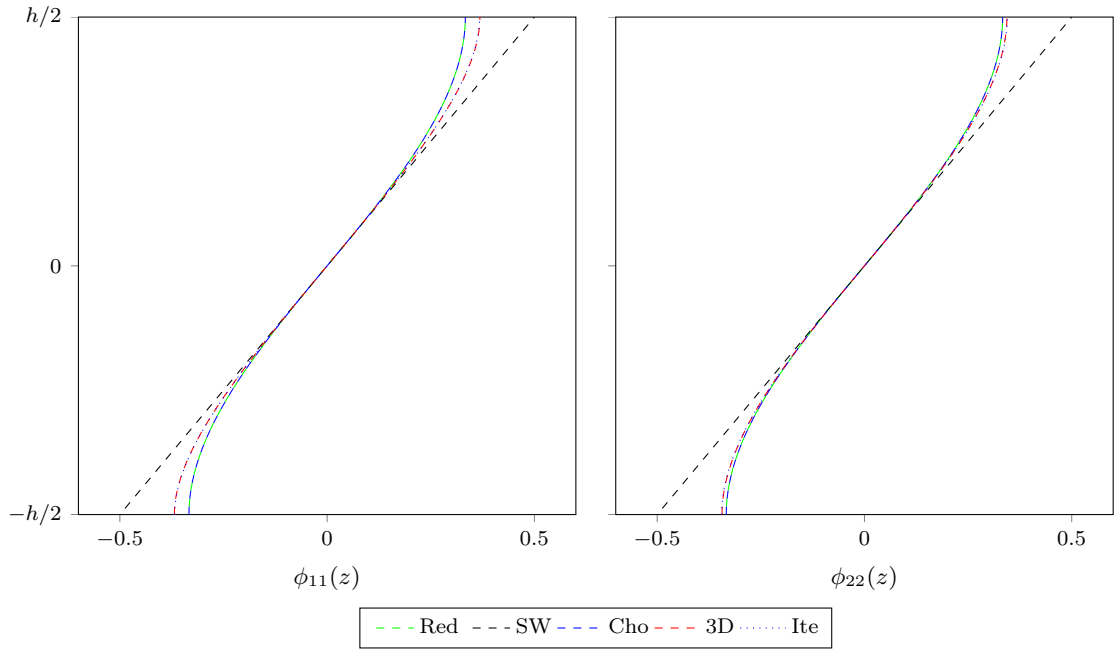

Figure 7: Transverse shear WF of the [0] single ply composite plate with $a/h = 4$ for each model.

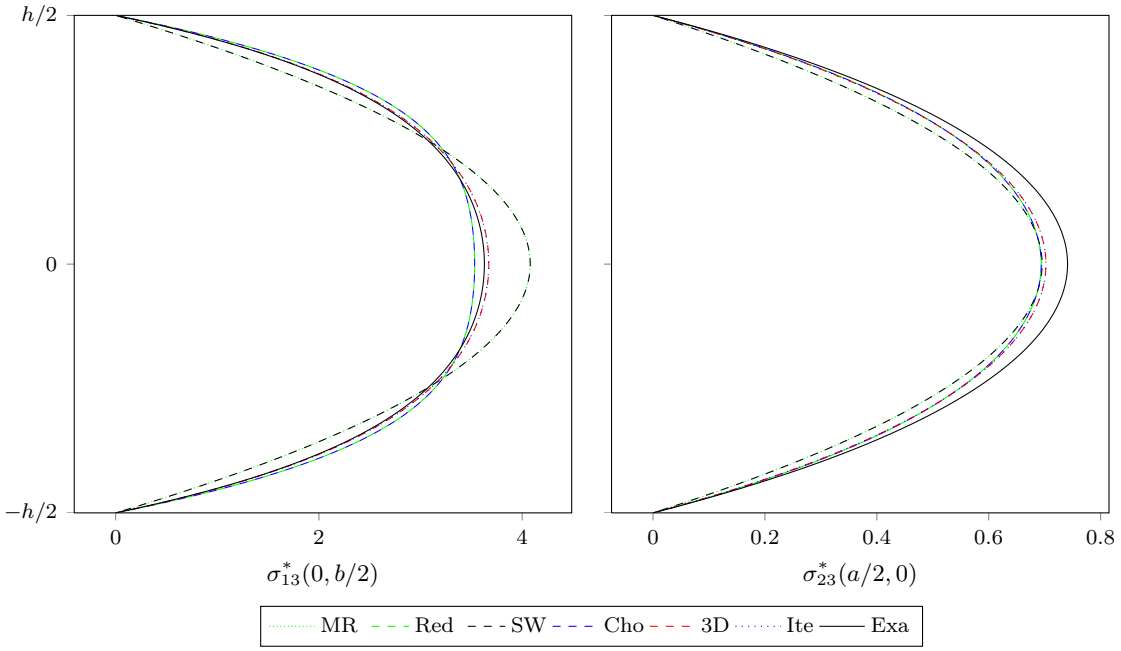

Figure 8: Nondimensionalized transverse shear stresses of the [0] single ply composite plate with $a/h = 4$ for each model.

Figure 9 shows the corresponding WF for $a/h = 4$, for all plate models except the MR. Figure 10 presents the transverse shear stresses at points A and B obtained for all models by the integration of equilibrium equations, compared to the exact solution, in the $a/h = 4$ case.

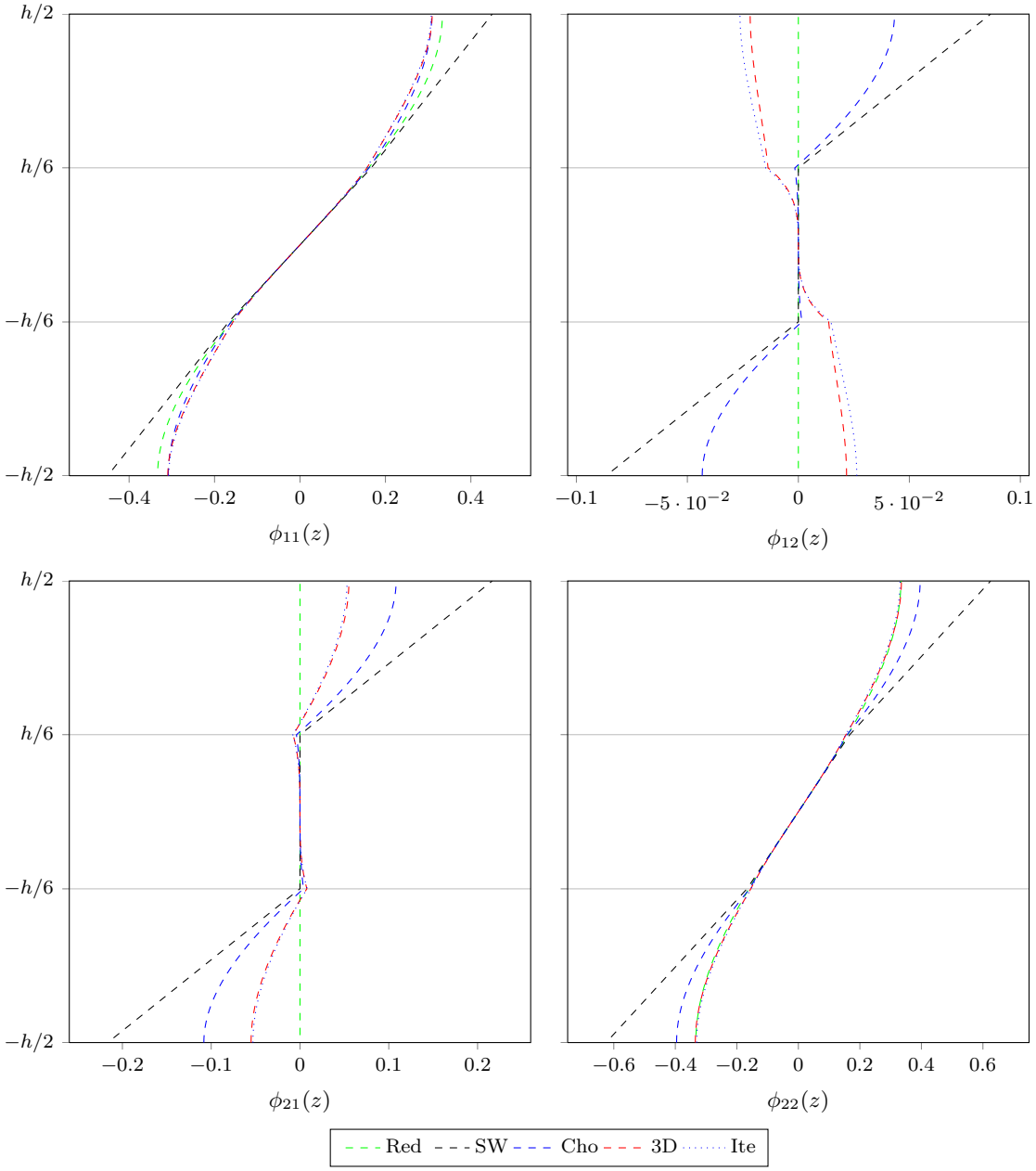

Figure 9: Transverse shear WF of the [0/30/0] composite plate with $a/h = 4$ for each model.

5.6. Discussion

The five studied cases have been chosen in order to represent a wide range of the laminates diversity. In addition to particular comments done for each case, general results may be issued from these studies. The MR model without the help of appropriate shear correction factors gives relatively poor values, except for thin plates. For moderately thick plates, Reddy's model is very accurate, except for the sandwich case because the high modulus ratio between layers is not properly managed by the model. On the contrary, the SW zig-zag linear model can manage it but fails for classical laminates, especially the single ply. Cho's model which *a priori* takes

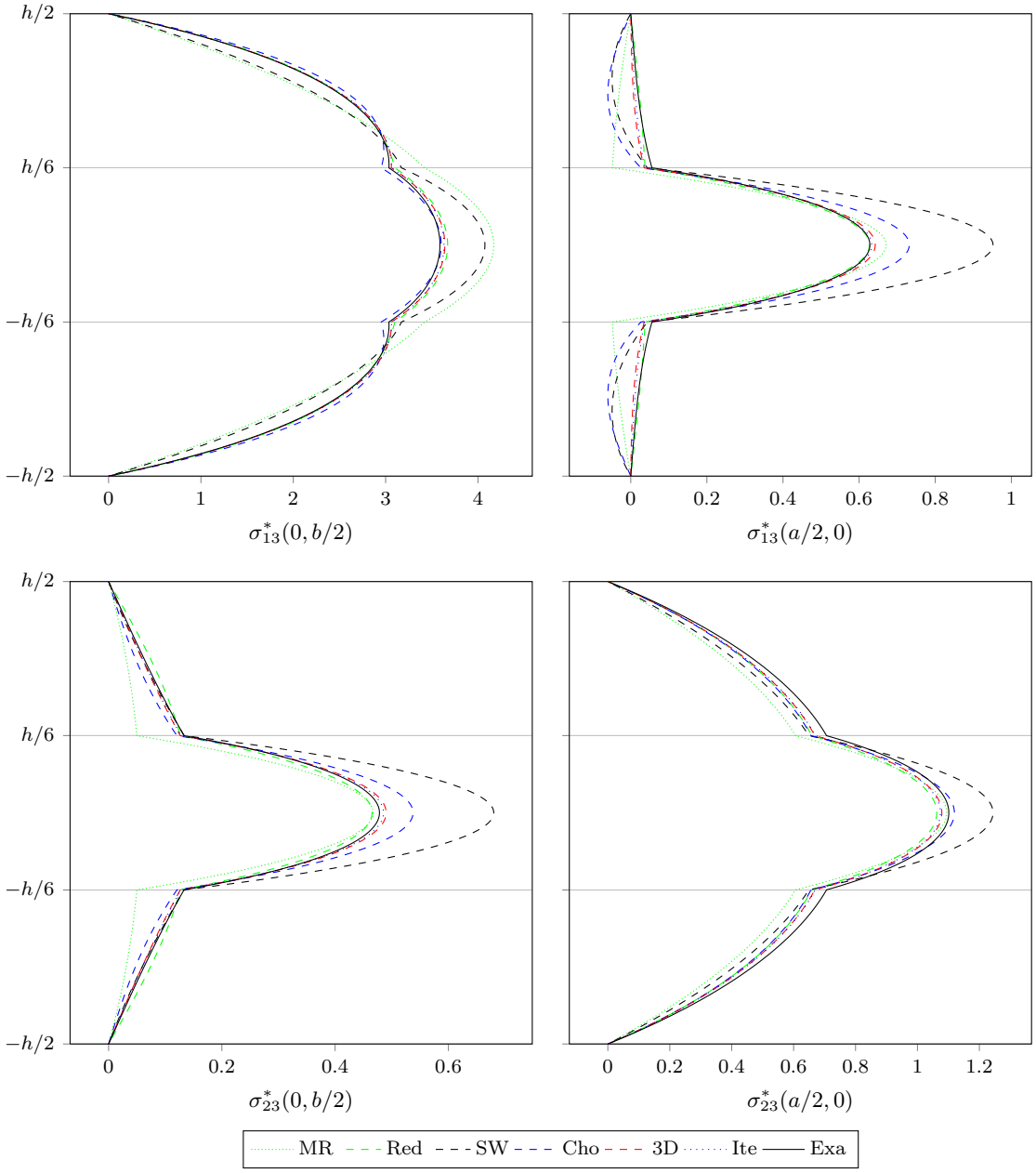

Figure 10: Nondimensionalized transverse shear stresses of the [0/30/0] composite plate with $a/h = 4$ for each model.

both advantage of a cubic variation coupled to a zig-zag variation of displacements gives sometimes poor values, especially for thick or very-thick plates. The Cho's model gives sometimes poor estimations, probably because the WF are too constrained by their formulation: as the cubic term is unique for all the layers, the functions adopt sometimes shapes that are not pertinent. In addition, its WF do not depend on the length-to-thickness ratio. Both present models, 3D and Ite, gives globally better results in all studied cases than other models. The Ite model seems to be the best of all. However, some values of the deflection are no so good. This is the reason why the Exa^2 solution has been introduced.

Indeed, all plate models presented in this study consider the generalized plane stress hypothesis, which consists on assuming $\sigma_{33} = 0$. This stress component is then eliminated from Hooke's law and a reduced Hooke's law with modified stiffnesses is issued from this process. This assumption is classically done in plate theories in order to manage the transition from 3D to 2D elasticity. For thin or moderately thick plates, this assumption is correct because moderate loadings on bottom and/or top faces of the plate cause bending, and then lead to in-plane stresses that over-exceed σ_{33}. For thick plates, the bending requires so high bottom and top loadings that the σ_{33} is no longer negligible.

Because all the presented models consider the generalized plane stress hypothesis, an exact solution Exa^2 involving the plane stress stiffnesses has been produced. It is really an exact solution, obtained with the same procedure than the Exa solution, which is described in Ref. [27], but for materials for which stiffnesses have been replaced by plane stress stiffnesses. As explained in the beginning of the section 5, it has been done by setting high values for E_3 (hence the corresponding compliance is negligible) and null values for ν_{13} and ν_{23}. Doing this makes Hooke's 3D stiffnesses coincide with the plane stress stiffnesses, except for round-off errors, and the exact solution procedure is usable without any modification.

The comparison for all models can now be done taking the Exa^2 exact solution as reference. It clearly shows that the Ite model surpasses all other models and is able to give almost the exact solution for deflection and transverse stresses, for all studied cases, and for all length to-thickness ratios. Fundamental frequencies however are not always exactly predicted by the Ite model, this may be explained by the fact that the successive integrations of equilibrium equations involved in the model have been done for the $\omega = 0$ frequency, hence further studies have to be done with emphasis for the dynamic behavior. Indeed, one may think that for higher frequencies the WF need to be modified.

Of course this spectacular result have to be replaced in the special context of this study. Plate problems solved in this study are simply supported problems with bi-sine loading. The WF used for the Ite model are obtained considering this special bending problem. Results show that the generic model is able to manage all lamination schemes if the good WF are provided, but there is no guarantee that WF obtained for this special bending configuration will work as well as for other configurations. The model with these WF may be a good candidate for other configurations, but others WF could perhaps be considered. Again, further studies need to be done in order to validate or adapt the Ite procedure to other configurations.

6. Conclusion

In this paper, a multilayered equivalent-single-layer plate theory based on warping functions (WF) has been presented. Two ways to generate the WF from three dimensional elasticity equations are described. The first one, called 3D, derives directly the WF from a 3D exact solution. The second one, called Ite, is an iterative process involving integrations of the equilibrium equations. Both process use the same core procedure which issues the WF from the variations of transverse shear stresses. The needed shear stresses variations are computed at the middle of the sides of the plate, for a simply supported bending problem with bi-sine load.

These two models are compared to other models and to the exact solution for five lamination sequences. Considered laminates plates are: a $[0/90/0]$ cross-ply rectangular plate, a square $[0/c/0]$ sandwich plate, a square $[0]$ single layer plate, a square $[-15/15]$ antisymmetric angle-ply plate, and a square plate with a more general $[0/30/0]$ lamination sequence. Models for comparison includes Mindlin-Reissner, Sun-Whitney, Reddy, and Kim-Cho models which have been also formulated in terms of WF, so the solution procedure is unique. The problem which is solved for comparison is the simply supported plate with bi-sine load, for which exact solutions are known. The comparisons are made on deflections, stresses and fundamental frequencies for length-to-thickness ratio varying from 2 to 100. The Mindlin-Reissner and Reddy models are not material-dependent, in other words, their WF are unique. In addition, $\varphi_{11}(z) = \varphi_{22}(z)$ and they never have non-null cross $\varphi_{12}(z)$

or $\varphi_{21}(z)$ WF. All other considered models have WF which depend on the properties of materials and on the lamination sequence, hence have 4 different WF for general lamination sequences.

Results show that for classical laminates – with moderate modulus ratio between layers – Reddy's model, which have cubic WF, is a good choice for thin and moderately thick plates, but is not so accurate for sandwich structures. On the contrary, Sun-Whitney model, which have zig-zag linear WF, is a good choice for the sandwich structure but is not enough accurate for classical laminates. Kim-Cho's model, which combines advantages from the two previous models, have cubic zig-zag WF. Its results are then better than those of previous models if the comparison is done on all class of laminates. However, it gives sometimes poor results for low length-to-thickness values, probably because the WF are too constrained by their formulation. Comparisons also show that the two presented models, 3D and Ite, gives globally better results than other tested models for all considered lamination sequences.

For the thick plates ($a/h \leq 4$), none of the models can be considered as accurate, even if the 3D and Ite models give better values on stresses and fundamental frequencies than other models. As all presented models consider the generalized plane stress hypothesis, an exact plane-stress solution called Exa^2 have been computed for all considered laminates, in order to make further comparisons. This has been done using the same 3D solution procedure after replacing stiffnesses of all materials with corresponding plane stress stiffnesses. Comparison with the Exa^2 reference clearly shows that the 3D and Ite models gives better results than other models. It can be seen that the Ite model gives exact values of deflection and stresses, and quasi-exact values for fundamental frequencies, for all laminates and for all length-to-thickness ratio values.

These last comparisons show clearly that the transverse deformation must be considered if thick plates have to be studied with equivalent-single-layer theories. It might also be the case for laminates which have high modulus ratio between layers, and for dynamic studies when the wavelength shortens. They also show that the generation of WF from an analytical solution or from the integration of equilibrium equations is a relatively easy way to have a very accurate universal model. Further studies must try to establish if the WF obtained by these methods are also pertinent for problems involving other boundary conditions, loading, or frequencies. If it is not the case, is there another way to compute pertinent WF, perhaps with a local approach ?

a/h	Model	w^*	%	%	$\sigma_{13}(B)$	%	%	$\sigma_{23}(A)$	%	%	ω^*	%	%
2	MR	6.6164	−18.98	−21.69	4.2978	+67.17	+64.28	0.54919	−17.76	−13.75	3.8633	+12.97	+13.01
	Red	7.8944	−3.32	−6.56	2.4649	−4.12	−5.78	0.59477	−10.93	−6.59	3.5335	+3.33	+3.36
	SW	7.8130	−4.32	−7.52	2.0026	−22.11	−23.45	0.66040	−1.11	+3.72	3.5485	+3.76	+3.80
	Cho	6.4960	−20.45	−23.11	1.4032	−45.42	−46.36	0.47682	−28.60	−25.11	3.8845	+13.59	+13.63
	3D	8.4451	+3.42	−0.04	2.6931	+4.76	+2.94	0.64111	−3.99	+0.69	3.4196	−0.00	+0.03
	Ite	8.4487	+3.46	−0.00	2.6163	+1.76	+0.00	0.63670	−4.65	+0.00	3.4186	−0.03	+0.00
	Exa^2	8.4488		*ref.*	2.6162		*ref.*	0.63670		*ref.*	3.4185		*ref.*
	Exa	8.1659	*ref.*		2.5709	*ref.*		0.66779	*ref.*		3.4197	*ref.*	
4	MR	2.0547	−27.17	−27.80	4.3625	+24.26	+24.05	0.25631	−23.18	−18.89	6.9503	+17.60	+17.64
	Red	2.6411	−6.38	−7.20	3.8253	+8.96	+8.78	0.30414	−8.84	−3.75	6.1331	+3.77	+3.80
	SW	2.7172	−3.68	−4.52	3.6580	+4.19	+4.02	0.31797	−4.70	+0.62	6.0461	+2.30	+2.33
	Cho	2.7331	−3.12	−3.96	3.2669	−6.95	−7.10	0.30071	−9.87	−4.84	6.0265	+1.97	+2.00
	3D	2.8459	+0.88	−0.00	3.5182	+0.21	+0.04	0.31616	−5.24	+0.05	5.9084	−0.03	+0.00
	Ite	2.8459	+0.88	−0.00	3.5167	+0.17	+0.00	0.31600	−5.29	+0.00	5.9084	−0.03	+0.00
	Exa^2	2.8459		*ref.*	3.5167		*ref.*	0.31600		*ref.*	5.9083		*ref.*
	Exa	2.8211	*ref.*		3.5108	*ref.*		0.33365	*ref.*		5.9100	*ref.*	
10	MR	0.75314	−18.04	−18.19	4.3895	+4.48	+4.48	0.13418	−11.94	−9.77	11.497	+10.47	+10.49
	Red	0.86219	−6.17	−6.34	4.2988	+2.32	+2.32	0.14468	−5.05	−2.71	10.750	+3.29	+3.31
	SW	0.88102	−4.12	−4.30	4.2687	+1.60	+1.61	0.14659	−3.80	−1.42	10.635	+2.19	+2.21
	Cho	0.91831	−0.07	−0.25	4.1841	−0.41	−0.41	0.14813	−2.79	−0.39	10.418	+0.10	+0.12
	3D	0.92059	+0.18	−0.00	4.2011	−0.01	−0.00	0.14871	−2.41	+0.00	10.405	−0.02	+0.00
	Ite	0.92059	+0.18	−0.00	4.2012	−0.00	+0.00	0.14871	−2.41	+0.00	10.405	−0.02	+0.00
	Exa^2	0.92059		*ref.*	4.2012		*ref.*	0.14870		*ref.*	10.405		*ref.*
	Exa	0.91891	*ref.*		4.2014	*ref.*		0.15237	*ref.*		10.408	*ref.*	
100	MR	0.50588	−0.35	−0.35	4.3952	+0.05	+0.05	0.10816	−0.18	−0.15	14.059	+0.18	+0.18
	Red	0.50700	−0.13	−0.13	4.3943	+0.03	+0.03	0.10827	−0.08	−0.04	14.043	+0.07	+0.07
	SW	0.50721	−0.09	−0.09	4.3940	+0.02	+0.02	0.10829	−0.06	−0.03	14.041	+0.05	+0.05
	Cho	0.50766	+0.00	−0.00	4.3931	−0.00	−0.00	0.10832	−0.04	−0.00	14.034	+0.00	+0.00
	3D	0.50767	+0.00	−0.00	4.3932	−0.00	+0.00	0.10832	−0.04	+0.00	14.034	−0.00	+0.00
	Ite	0.50767	+0.00	−0.00	4.3932	−0.00	+0.00	0.10832	−0.04	+0.00	14.034	−0.00	+0.00
	Exa^2	0.50767		*ref.*	4.3932		*ref.*	0.10832		*ref.*	14.034		*ref.*
	Exa	0.50766	*ref.*		4.3932	*ref.*		0.10836	*ref.*		14.034	*ref.*	

Table 2: Comparison between the different models for the rectangular [0/90/0] composite plate with a varying length-to-thickness ratio.

a/h	Model	w^*	%	%	$\sigma_{13}(B)$	%	%	$\sigma_{23}(A)$	%	%	ω^*	%	%
2	MR	0.50904	−44.74	−44.07	2.5177	+31.01	+35.10	1.0476	−30.40	−24.36	6.9339	+29.88	+31.57
	Red	0.85344	−7.34	−6.23	1.9150	−0.35	+2.76	1.3300	−11.65	−3.97	5.4307	+1.72	+3.04
	SW	0.90224	−2.05	−0.86	1.8459	−3.95	−0.95	1.3963	−7.24	+0.82	5.2900	−0.92	+0.37
	Cho	0.88896	−3.49	−2.32	1.8320	−4.67	−1.70	1.3570	−9.85	−2.02	5.3281	−0.20	+1.10
	3D	0.90894	−1.32	−0.13	1.8562	−3.41	−0.40	1.3795	−8.36	−0.40	5.2730	−1.23	+0.05
	Ite	0.91010	−1.19	−0.00	1.8636	−3.02	+0.00	1.3850	−7.99	+0.00	5.2703	−1.28	+0.00
	Exa[2]	0.91010		*ref.*	1.8636		*ref.*	1.3850		*ref.*	5.2702		*ref.*
	Exa	0.92108	*ref.*		1.9217	*ref.*		1.5053	*ref.*		5.3389	*ref.*	
4	MR	0.16645	−45.57	−45.67	2.8525	+18.99	+19.09	0.69992	−36.72	−34.02	12.233	+33.77	+34.67
	Red	0.28349	−7.30	−7.47	2.4657	+2.85	+2.94	1.0011	−9.49	−5.63	9.4350	+3.17	+3.86
	SW	0.30453	−0.42	−0.60	2.3971	−0.01	+0.08	1.0651	−3.70	+0.41	9.1084	−0.40	+0.27
	Cho	0.30416	−0.54	−0.72	2.3897	−0.32	−0.23	1.0560	−4.52	−0.45	9.1152	−0.33	+0.34
	3D	0.30636	+0.18	−0.01	2.3947	−0.11	−0.02	1.0603	−4.13	−0.04	9.0843	−0.67	+0.00
	Ite	0.30638	+0.19	−0.00	2.3952	−0.09	+0.00	1.0607	−4.09	+0.00	9.0840	−0.67	+0.00
	Exa[2]	0.30638		*ref.*	2.3952		*ref.*	1.0607		*ref.*	9.0840		*ref.*
	Exa	0.30581	*ref.*		2.3973	*ref.*		1.1060	*ref.*		9.1452	*ref.*	
10	MR	0.057970	−34.15	−34.25	3.1506	+5.10	+5.00	0.39042	−26.89	−25.45	21.096	+22.82	+23.06
	Red	0.082517	−6.27	−6.41	3.0293	+1.05	+0.96	0.49783	−6.77	−4.95	17.716	+3.14	+3.35
	SW	0.087730	−0.34	−0.50	3.0029	+0.17	+0.08	0.52287	−2.08	−0.16	17.185	+0.05	+0.25
	Cho	0.087908	−0.14	−0.30	3.0001	+0.08	−0.01	0.52265	−2.12	−0.20	17.168	−0.05	+0.15
	3D	0.088171	+0.16	−0.00	3.0005	+0.09	−0.00	0.52371	−1.93	−0.00	17.143	−0.20	+0.00
	Ite	0.088172	+0.16	−0.00	3.0005	+0.09	+0.00	0.52373	−1.92	−0.00	17.143	−0.20	+0.00
	Exa[2]	0.088172		*ref.*	3.0005		*ref.*	0.52373		*ref.*	17.143		*ref.*
	Exa	0.088033	*ref.*		2.9978	*ref.*		0.53399	*ref.*		17.177	*ref.*	
100	MR	0.035362	−0.93	−0.94	3.2418	+0.06	+0.06	0.29572	−0.60	−0.56	27.275	+0.47	+0.47
	Red	0.035631	−0.18	−0.18	3.2404	+0.01	+0.01	0.29705	−0.15	−0.12	27.172	+0.09	+0.09
	SW	0.035691	−0.01	−0.01	3.2400	+0.00	+0.00	0.29738	−0.05	−0.01	27.149	+0.00	+0.01
	Cho	0.035694	−0.00	−0.01	3.2400	+0.00	+0.00	0.29738	−0.04	−0.00	27.148	+0.00	+0.00
	3D	0.035697	+0.00	−0.00	3.2400	+0.00	+0.00	0.29740	−0.04	−0.00	27.147	−0.00	−0.00
	Ite	0.035697	+0.00	−0.00	3.2400	+0.00	+0.00	0.29740	−0.04	−0.00	27.147	−0.00	−0.00
	Exa[2]	0.035697		*ref.*	3.2400		*ref.*	0.29740		*ref.*	27.147		*ref.*
	Exa	0.035695	*ref.*		3.2399	*ref.*		0.29751	*ref.*		27.148	*ref.*	

Table 3: Comparison between the different models for the square $[0/c/0]$ sandwich plate with a varying length-to-thickness ratio.

a/h	Model	w^*	%	%	$\sigma_{13}(B)$	%	%	$\sigma_{23}(A)$	%	%	$\sigma_{23}(D)$	%	%	$\sigma_{13}(C)$	%	%	ω^*	%	%
2	MR	4.3448	−4.61	−10.46	2.5852	+10.45	+9.02	0.96150	−8.99	−4.02	0.39006	+6.66	+2.00	1.2538	+132.50	+103.37	4.7206	+5.62	+5.70
	Red	4.3111	−5.35	−11.15	1.2945	−44.70	−45.41	0.66314	−37.23	−33.80	0.61086	+67.03	+59.73	1.7362	+221.94	+181.61	4.7611	+6.52	+6.61
	SW	3.8609	−15.24	−20.43	1.5621	−33.26	−34.13	0.82808	−21.62	−17.34	0.77361	+111.53	+102.29	2.3751	+340.42	+285.24	4.9993	+11.85	+11.94
	Cho	3.9838	−12.54	−17.90	0.68465	−70.75	−71.13	0.58472	−44.65	−41.63	0.85309	+133.26	+123.07	2.4671	+357.48	+300.16	4.9478	+10.70	+10.79
	3D	4.8406	+6.28	−0.24	2.3183	−0.96	−2.24	0.93896	−11.12	−6.27	0.41381	+13.15	+8.21	0.85886	+59.26	+39.31	4.4826	+0.29	+0.37
	Ite	4.8523	+6.53	−0.00	2.3720	+1.34	+0.03	1.0020	−5.15	+0.03	0.38223	+4.51	−0.05	0.61566	+14.16	−0.14	4.4706	+0.03	+0.10
	Exa^2	4.8524		*ref.*	2.3713		*ref.*	1.0018		*ref.*	0.38243		*ref.*	0.61652		*ref.*	4.4660		*ref.*
	Exa	4.5548	*ref.*		2.3407	*ref.*		1.0565	*ref.*		0.36572	*ref.*		0.53928	*ref.*		4.4695	*ref.*	
4	MR	1.5762	−7.60	−9.49	2.7968	+3.47	+3.29	0.77953	−9.30	−5.53	0.40374	+2.37	+1.35	1.1382	+36.90	+34.50	7.7953	+4.57	+4.88
	Red	1.6594	−2.73	−4.72	2.4047	−11.04	−11.19	0.72164	−16.03	−12.55	0.46519	+17.96	+16.78	1.2815	+54.14	+51.43	7.6323	+2.38	+2.69
	SW	1.5082	−11.59	−13.40	2.5237	−6.63	−6.79	0.76061	−11.50	−7.83	0.50488	+28.02	+26.74	1.4053	+69.03	+66.06	7.9690	+6.90	+7.22
	Cho	1.6197	−5.05	−7.00	2.2063	−18.38	−18.52	0.70919	−17.48	−14.06	0.53761	+36.32	+34.96	1.4786	+77.85	+74.72	7.7273	+3.66	+3.97
	3D	1.7414	+2.08	−0.01	2.6980	−0.19	−0.36	0.81709	−4.93	−0.98	0.40205	+1.95	+0.93	0.86867	+4.48	+2.65	7.4376	−0.23	+0.07
	Ite	1.7416	+2.09	−0.00	2.7078	+0.17	+0.00	0.82521	−3.98	+0.00	0.39835	+1.01	−0.00	0.84627	+1.79	−0.00	7.4354	−0.26	+0.04
	Exa^2	1.7416		*ref.*	2.7077		*ref.*	0.82520		*ref.*	0.39836		*ref.*	0.84627		*ref.*	7.4324		*ref.*
	Exa	1.7059	*ref.*		2.7031	*ref.*		0.85945	*ref.*		0.39437	*ref.*		0.83139	*ref.*		7.4548	*ref.*	
10	MR	0.77629	−3.29	−3.77	2.9520	+0.67	+0.62	0.64607	−3.11	−1.97	0.41376	+0.54	+0.38	1.0534	+6.32	+6.18	11.218	+1.74	+1.87
	Red	0.79522	−0.93	−1.42	2.8811	−1.74	−1.79	0.64072	−3.92	−2.79	0.42393	+3.02	+2.85	1.0791	+8.92	+8.77	11.093	+0.60	+0.73
	SW	0.76841	−4.27	−4.75	2.9075	−0.84	−0.89	0.64468	−3.32	−2.18	0.43019	+4.54	+4.36	1.0933	+10.34	+10.19	11.275	+2.26	+2.39
	Cho	0.79198	−1.34	−1.82	2.8463	−2.93	−2.98	0.64029	−3.98	−2.85	0.43619	+6.00	+5.82	1.1098	+12.01	+11.86	11.116	+0.81	+0.94
	3D	0.80669	+0.49	−0.00	2.9334	+0.04	−0.01	0.65877	−1.21	−0.05	0.41233	+0.20	+0.03	0.99287	+0.21	+0.07	11.012	−0.13	+0.00
	Ite	0.80669	+0.49	−0.00	2.9337	+0.05	+0.00	0.65908	−1.16	−0.00	0.41220	+0.17	+0.00	0.99215	+0.13	+0.00	11.012	−0.13	+0.00
	Exa^2	0.80669		*ref.*	2.9337		*ref.*	0.65908		*ref.*	0.41220		*ref.*	0.99214		*ref.*	11.012		*ref.*
	Exa	0.80272	*ref.*		2.9323	*ref.*		0.66683	*ref.*		0.41152	*ref.*		0.99081	*ref.*		11.026	*ref.*	
100	MR	0.62204	−0.04	−0.05	2.9945	+0.01	+0.01	0.60954	−0.04	−0.02	0.41651	+0.01	+0.00	1.0302	+0.06	+0.06	12.677	+0.02	+0.03
	Red	0.62224	−0.01	−0.02	2.9937	−0.02	−0.02	0.60950	−0.04	−0.03	0.41661	+0.03	+0.03	1.0305	+0.09	+0.09	12.675	+0.01	+0.01
	SW	0.62197	−0.06	−0.06	2.9940	−0.01	−0.01	0.60953	−0.04	−0.03	0.41667	+0.05	+0.04	1.0306	+0.10	+0.10	12.678	+0.03	+0.03
	Cho	0.62222	−0.02	−0.02	2.9934	−0.03	−0.03	0.60950	−0.04	−0.03	0.41673	+0.06	+0.06	1.0308	+0.12	+0.12	12.675	+0.01	+0.01
	3D	0.62235	+0.01	−0.00	2.9943	+0.00	+0.00	0.60969	−0.01	−0.00	0.41649	+0.00	+0.00	1.0296	+0.00	+0.00	12.674	−0.00	+0.00
	Ite	0.62235	+0.01	−0.00	2.9943	+0.00	+0.00	0.60969	−0.01	−0.00	0.41649	+0.00	+0.00	1.0296	+0.00	+0.00	12.674	−0.00	+0.00
	Exa^2	0.62235		*ref.*	2.9943		*ref.*	0.60969		*ref.*	0.41649		*ref.*	1.0296		*ref.*	12.674		*ref.*
	Exa	0.62232	*ref.*		2.9942	*ref.*		0.60978	*ref.*		0.41648	*ref.*		1.0296	*ref.*		12.674	*ref.*	

Table 4: Comparison between the different models for the square [−15/15] composite plate with a varying length-to-thickness ratio.

a/h	Model	w^*	%	%	$\sigma_{13}(B)$	%	%	$\sigma_{23}(A)$	%	%	ω^*	%	%
2	MR	4.3108	−3.63	−9.94	3.7502	+31.36	+24.72	1.0244	+2.65	+8.26	4.7281	+4.85	+5.05
	Red	4.5262	+1.19	−5.44	2.0291	−28.93	−32.52	0.85739	−14.09	−9.39	4.6223	+2.50	+2.70
	SW	4.3108	−3.63	−9.94	3.7502	+31.36	+24.72	1.0244	+2.65	+8.26	4.7281	+4.85	+5.05
	Cho	4.5262	+1.19	−5.44	2.0291	−28.93	−32.52	0.85739	−14.09	−9.39	4.6223	+2.50	+2.70
	3D	4.7804	+6.87	−0.13	3.1758	+11.24	+5.62	0.95157	−4.65	+0.56	4.5040	−0.12	+0.07
	Ite	4.7861	+7.00	−0.01	3.0077	+5.35	+0.03	0.94628	−5.18	+0.00	4.5009	−0.19	+0.00
	Exa^2	4.7864		*ref.*	3.0069		*ref.*	0.94624		*ref.*	4.5007		*ref.*
	Exa	4.4730	*ref.*		2.8549	*ref.*		0.99796	*ref.*		4.5093	*ref.*	
4	MR	1.4643	−8.42	−10.16	4.0792	+12.44	+11.18	0.69540	−6.14	−0.98	8.1438	+5.17	+5.34
	Red	1.6206	+1.35	−0.57	3.5324	−2.63	−3.72	0.69382	−6.35	−1.21	7.7522	+0.11	+0.28
	SW	1.4643	−8.42	−10.16	4.0792	+12.44	+11.18	0.69540	−6.14	−0.98	8.1438	+5.17	+5.34
	Cho	1.6206	+1.35	−0.57	3.5324	−2.63	−3.72	0.69382	−6.35	−1.21	7.7522	+0.11	+0.28
	3D	1.6298	+1.93	−0.00	3.6718	+1.21	+0.08	0.70227	−5.21	−0.00	7.7311	−0.16	+0.00
	Ite	1.6298	+1.93	−0.00	3.6693	+1.14	+0.01	0.70231	−5.21	+0.00	7.7311	−0.16	+0.00
	Exa^2	1.6299		*ref.*	3.6690		*ref.*	0.70231		*ref.*	7.7310		*ref.*
	Exa	1.5989	*ref.*		3.6280	*ref.*		0.74089	*ref.*		7.7436	*ref.*	
10	MR	0.60418	−4.82	−5.17	4.3281	+2.50	+2.32	0.44658	−3.85	−1.85	12.795	+2.59	+2.66
	Red	0.63709	+0.37	−0.01	4.2249	+0.06	−0.12	0.45479	−2.08	−0.05	12.464	−0.06	+0.00
	SW	0.60418	−4.82	−5.17	4.3281	+2.50	+2.32	0.44658	−3.85	−1.85	12.795	+2.59	+2.66
	Cho	0.63709	+0.37	−0.01	4.2249	+0.06	−0.12	0.45479	−2.08	−0.05	12.464	−0.06	+0.00
	3D	0.63714	+0.37	−0.00	4.2300	+0.18	−0.00	0.45499	−2.03	−0.00	12.463	−0.06	+0.00
	Ite	0.63714	+0.37	−0.00	4.2301	+0.18	+0.00	0.45500	−2.03	−0.00	12.463	−0.06	+0.00
	Exa^2	0.63715		*ref.*	4.2300		*ref.*	0.45500		*ref.*	12.463		*ref.*
	Exa	0.63477	*ref.*		4.2223	*ref.*		0.46444	*ref.*		12.471	*ref.*	
100	MR	0.43300	−0.08	−0.08	4.3973	+0.03	+0.02	0.37735	−0.06	−0.03	15.196	+0.04	+0.04
	Red	0.43335	+0.00	−0.00	4.3962	+0.00	−0.00	0.37746	−0.03	−0.00	15.190	−0.00	−0.00
	SW	0.43300	−0.08	−0.08	4.3973	+0.03	+0.02	0.37735	−0.06	−0.03	15.196	+0.04	+0.04
	Cho	0.43335	+0.00	−0.00	4.3962	+0.00	−0.00	0.37746	−0.03	−0.00	15.190	−0.00	−0.00
	3D	0.43335	+0.00	−0.00	4.3962	+0.00	+0.00	0.37746	−0.03	−0.00	15.190	−0.00	+0.00
	Ite	0.43335	+0.00	−0.00	4.3962	+0.00	+0.00	0.37746	−0.03	−0.00	15.190	−0.00	+0.00
	Exa^2	0.43335		*ref.*	4.3962		*ref.*	0.37746		*ref.*	15.190		*ref.*
	Exa	0.43333	*ref.*		4.3961	*ref.*		0.37756	*ref.*		15.190	*ref.*	

Table 5: Comparison between the different models for the square [0] single ply composite plate with a varying length-to-thickness ratio.

a/h	Model	w^*	%	%	$\sigma_{13}(B)$	%	%	$\sigma_{23}(A)$	%	%	$\sigma_{23}(B)$	%	%	$\sigma_{13}(A)$	%	%	ω^*	%	%
2	MR	4.3307	−7.30	−13.36	3.9829	+46.15	+38.02	1.5415	+15.29	+15.38	0.61354	+16.99	+8.40	0.87873	+32.75	+24.61	4.7242	+7.21	+7.47
	Red	4.7450	+1.57	−5.07	2.3244	−14.71	−19.45	1.1334	−15.23	−15.16	0.39166	−25.32	−30.80	0.48255	−27.10	−31.57	4.4994	+2.11	+2.35
	SW	4.4049	−5.71	−11.87	3.8213	+40.22	+32.42	1.9621	+46.75	+46.87	1.1894	+126.78	+110.13	1.7529	+164.81	+148.57	4.6683	+5.94	+6.19
	Cho	4.5986	−1.56	−8.00	2.3230	−14.76	−19.50	1.3101	−2.02	−1.94	0.57580	+9.79	+1.73	0.90351	+36.49	+28.12	4.5753	+3.83	+4.08
	3D	4.9868	+6.74	−0.23	3.1129	+14.22	+7.87	1.4246	+6.55	+6.64	0.64957	+23.86	+14.76	0.86657	+30.91	+22.89	4.4067	+0.01	+0.24
	Ite	4.9982	+6.99	−0.00	2.8858	+5.89	+0.00	1.3360	−0.08	+0.00	0.56602	+7.93	+0.00	0.70518	+6.53	−0.00	4.3977	−0.20	+0.04
	Exa[2]	4.9983		*ref.*	2.8857		*ref.*	1.3360		*ref.*	0.56601		*ref.*	0.70519		*ref.*	4.3960		*ref.*
	Exa	4.6717	*ref.*		2.7253	*ref.*		1.3370	*ref.*		0.52445	*ref.*		0.66195	*ref.*		4.4064	*ref.*	
4	MR	1.4728	−13.63	−15.24	4.1710	+16.24	+14.82	1.0945	−0.61	+1.89	0.46704	−2.34	−3.79	0.67093	+6.79	+5.95	8.1258	+8.40	+8.58
	Red	1.7025	−0.15	−2.02	3.6717	+2.32	+1.07	1.0624	−3.53	−1.11	0.46523	−2.72	−4.16	0.62730	−0.16	−0.94	7.5603	+0.86	+1.03
	SW	1.5616	−8.42	−10.13	4.0752	+13.57	+12.18	1.2440	+12.96	+15.80	0.68005	+42.20	+40.09	0.95180	+51.49	+50.31	7.8819	+5.15	+5.32
	Cho	1.7138	+0.51	−1.37	3.6017	+0.37	−0.85	1.1193	+1.63	+4.19	0.53754	+12.40	+10.74	0.73172	+16.46	+15.55	7.5351	+0.52	+0.69
	3D	1.7376	+1.90	−0.00	3.6411	+1.47	+0.23	1.0788	−2.05	+0.42	0.49005	+2.47	+0.95	0.64235	+2.24	+1.44	7.4846	−0.15	+0.01
	Ite	1.7376	+1.91	−0.00	3.6327	+1.24	+0.00	1.0743	−2.45	+0.00	0.48544	+1.51	+0.00	0.63325	+0.79	+0.00	7.4841	−0.16	+0.01
	Exa[2]	1.7376		*ref.*	3.6327		*ref.*	1.0743		*ref.*	0.48543		*ref.*	0.63324		*ref.*	7.4836		*ref.*
	Exa	1.7051	*ref.*		3.5883	*ref.*		1.1013	*ref.*		0.47822	*ref.*		0.62828	*ref.*		7.4961	*ref.*	
10	MR	0.59918	−8.29	−8.63	4.3112	+3.04	+2.85	0.74022	−2.55	−1.48	0.32843	−4.09	−4.20	0.51166	−0.21	−0.30	12.850	+4.51	+4.58
	Red	0.64701	−0.97	−1.34	4.2213	+0.89	+0.70	0.75108	−1.12	−0.03	0.34034	−0.62	−0.73	0.51673	+0.78	+0.69	12.370	+0.61	+0.67
	SW	0.62084	−4.98	−5.33	4.2884	+2.49	+2.30	0.77032	+1.41	+2.53	0.37135	+8.44	+8.32	0.57195	+11.55	+11.45	12.625	+2.68	+2.75
	Cho	0.65454	+0.18	−0.19	4.1991	+0.36	+0.17	0.76235	+0.36	+1.47	0.35476	+3.59	+3.47	0.53317	+3.98	+3.89	12.299	+0.03	+0.10
	3D	0.65579	+0.37	−0.00	4.1920	+0.19	+0.00	0.75140	−1.08	+0.01	0.34297	+0.15	+0.04	0.51344	+0.14	+0.05	12.287	−0.06	+0.00
	Ite	0.65579	+0.37	−0.00	4.1919	+0.19	+0.00	0.75131	−1.09	+0.00	0.34285	+0.12	+0.00	0.51321	+0.09	+0.00	12.287	−0.06	+0.00
	Exa[2]	0.65579		*ref.*	4.1919		*ref.*	0.75131		*ref.*	0.34285		*ref.*	0.51320		*ref.*	12.287		*ref.*
	Exa	0.65337	*ref.*		4.1841	*ref.*		0.75958	*ref.*		0.34245	*ref.*		0.51275	*ref.*		12.295	*ref.*	
100	MR	0.42339	−0.14	−0.14	4.3503	+0.03	+0.03	0.63890	−0.04	−0.03	0.28614	−0.07	−0.07	0.47133	−0.01	−0.01	15.367	+0.07	+0.07
	Red	0.42390	−0.02	−0.02	4.3494	+0.01	+0.01	0.63907	−0.02	−0.00	0.28630	−0.01	−0.01	0.47142	+0.01	+0.01	15.358	+0.01	+0.01
	SW	0.42363	−0.08	−0.09	4.3501	+0.03	+0.02	0.63922	+0.01	+0.02	0.28660	+0.09	+0.09	0.47203	+0.14	+0.14	15.363	+0.04	+0.04
	Cho	0.42399	+0.00	−0.00	4.3491	+0.00	+0.00	0.63919	+0.00	+0.02	0.28646	+0.04	+0.04	0.47159	+0.05	+0.05	15.356	+0.00	+0.00
	3D	0.42400	+0.00	−0.00	4.3490	+0.00	+0.00	0.63907	−0.01	+0.00	0.28633	+0.00	+0.00	0.47137	+0.00	+0.00	15.356	−0.00	+0.00
	Ite	0.42400	+0.00	−0.00	4.3490	+0.00	+0.00	0.63907	−0.01	+0.00	0.28633	+0.00	+0.00	0.47137	+0.00	+0.00	15.356	−0.00	+0.00
	Exa[2]	0.42400		*ref.*	4.3490		*ref.*	0.63907		*ref.*	0.28633		*ref.*	0.47137		*ref.*	15.356		*ref.*
	Exa	0.42398	*ref.*		4.3490	*ref.*		0.63917	*ref.*		0.28633	*ref.*		0.47136	*ref.*		15.356	*ref.*	

Table 6: Comparison between the different models for the square [0/30/0] composite plate with a varying length-to-thickness ratio.

[1] G. Kirchhoff. Ueber das gleichgewicht und die bewegung einer elastischen scheibe (in German). *Crelle Journal fur die reine und angewandte Mathematik*, 40:51–88, 1850.
[2] A. E. H. Love. On the small free vibrations and deformations of elastic shells. *Philosophical trans. of the Royal Society (London) A*, 179:491–546, jan 1888.
[3] J. W. S. Rayleigh. *The Theory of Sound (republication of the 1894 second edition) – vol. 1.* Macmillan, 1944.
[4] E. Reissner. The effect of transverse shear deformation on the bending of elastic plates. *Journal of Applied Mechanics*, 12:69–77, 1945.
[5] Y. S. Uflyand. The propagation of waves in the transverse vibrations of bars and plates (in Russian). *Akad. Nauk. SSSR, Prikl. Mat. Mech.*, 12:287–300, 1948.
[6] R. D. Mindlin. Influence of rotatory inertia and shear on flexural motions of isotropic, elastic plates. *Journal of Applied Mechanics*, 18:31–38, 1951.
[7] J. M. Whitney. Shear correction factors for orthotropic laminates under static load. *Journal of Applied Mechanics*, 40(1):302–304, mar 1973.
[8] Ahmed K. Noor and W. Scott Burton. Stress and free vibration analyses of multilayered composite plates. *Composite Structures*, 11(3):183–204, 1989.
[9] Perngjin F. Pai. A new look at shear correction factors and warping functions of anisotropic laminates. *International Journal of Solids and Structures*, 32(16):2295–2313, 1995.
[10] E. Carrera. Theories and finite elements for multilayered, anisotropic, composite plates and shells. *Archives of Computational Methods in Engineering*, 9:87–140, 2002. 10.1007/BF02736649.
[11] J. N. Reddy. A simple higher-order theory for laminated composite plates. *Journal of Applied Mechanics*, 51(4):745–752, 1984.
[12] M. Touratier. An efficient standard plate theory. *International Journal of Engineering Science*, 29(8):901–916, 1991.
[13] K. P. Soldatos. A transverse shear deformation theory for homogeneous monoclinic plates. *Acta Mechanica*, 94(3-4):195–220, September 1992.
[14] Chien H. Thai, A.J.M. Ferreira, S.P.A. Bordas, T. Rabczuk, and H. Nguyen-Xuan. Isogeometric analysis of laminated composite and sandwich plates using a new inverse trigonometric shear deformation theory. *European Journal of Mechanics - A/Solids*, 201x.
[15] S. G. Lekhnitskii. Strength calculation of composite beams. *Vestn. Inzh. Tekh.*, 9, 1935.
[16] S. A. Ambartsumyan. On a general theory of bending of anisotropic plates. *Investiia Akad. Nauk SSSR Ot Tekh. Nauk*, 4, 1958.
[17] J. M. Whitney. The effect of transverse shear deformation on the bending of laminated plates. *Journal of Composite Materials*, 3(3):534–547, July 1969.
[18] C. T. Sun and J. M. Whitney. Theories for the dynamic response of laminated plates. *AIAA Journal*, 11:178–183, 1973.
[19] Maenghyo Cho and R. R. Parmerter. Efficient higher order composite plate theory for general lamination configurations. *AIAA Journal*, 31:1299–1306, July 1993.
[20] Hemendra Arya, R.P. Shimpi, and N.K. Naik. A zigzag model for laminated composite beams. *Composite Structures*, 56(1):21–24, April 2002.
[21] Jun-Sik Kim and Maenghyo Cho. Enhanced modeling of laminated and sandwich plates via strain energy transformation. *Composites Science and Technology*, 66(11–12):1575–1587, 2006.
[22] C. Wanji and W. Zhen. A selective review on recent development of displacement-based laminated plate theories. *Recent Patents Mech. Engng*, 1:29–44, 2008.
[23] Rasoul Khandan, Siamak Noroozi, Philip Sewell, and John Vinney. The development of laminated composite plate theories: a review. *Journal of Materials Science*, 47(16):5901–5910, February 2012.
[24] A. Loredo and A. Castel. A multilayer anisotropic plate model with warping functions for the study of vibrations reformulated from woodcock's work. *Journal of Sound and Vibration*, 332(1):102–125, 2013.
[25] Pagano NJ. Exact solutions for rectangular bidirectional composites and sandwich plates. *Journal of Composite Materials*, 4:20–34, 1970.
[26] S. Srinivas, C.V. Joga Rao, and A.K. Rao. An exact analysis for vibration of simply-supported homogeneous and laminated thick rectangular plates. *Journal of Sound and Vibration*, 12(2):187–199, June 1970.
[27] A. Loredo. Exact 3D solution for static and damped harmonic response of simply supported general laminates. *Composite Structures*, 108:625–634, February 2014.
[28] Ahmed K. Noor and W. Scott Burton. Three-dimensional solutions for antisymmetrically laminated anisotropic plates. *Journal of Applied Mechanics*, 57(1):182–188, March 1990.
[29] A. Loredo. Etude bibliographique sur les théories des plaques et implantation d'une formulation sur un élément fini. Pre-doctoral research report (in french), jun 1989.
[30] Roland L. Woodcock. Free vibration of advanced anisotropic multilayered composites with arbitrary boundary conditions. *Journal of Sound and Vibration*, 312(4–5):769–788, may 2008.
[31] Jun-Sik Kim and Maenghyo Cho. Enhanced first-order theory based on mixed formulation and transverse normal effect. *International Journal of Solids and Structures*, 44(3–4):1256–1276, February 2007.

Appendix A. Appendices

Appendix A.1. Detailed formulation of the stiffness and mass matrices

$$K = \begin{bmatrix} K_1 & K_2 \\ K_3 & K_4 \end{bmatrix} \qquad \text{and} \qquad M = \begin{bmatrix} M_1 & M_2 \\ M_3 & M_4 \end{bmatrix} \qquad \text{with} \tag{A.1}$$

$$K_1 = \begin{bmatrix} -A_{1212}\eta^2 - A_{1111}\xi^2 & -A_{1122}\xi\eta - A_{1212}\xi\eta & B_{1122}\xi\eta^2 + 2B_{1212}\xi\eta^2 + B_{1111}\xi^3 & -E_{1111}\xi^2 - E_{1221}\eta^2 & -E_{1112}\xi\eta - E_{1222}\xi\eta \\ -A_{1122}\xi\eta - A_{1212}\xi\eta & -A_{2222}\eta^2 - A_{1212}\xi^2 & B_{2222}\eta^3 + B_{1122}\xi^2\eta + 2B_{1212}\xi^2\eta & -E_{2211}\xi\eta - E_{1221}\xi\eta & -E_{1222}\xi^2 - E_{2212}\eta^2 \\ B_{1122}\xi\eta^2 + 2B_{1212}\xi\eta^2 + B_{1111}\xi^3 & B_{2222}\eta^3 + B_{1122}\xi^2\eta + 2B_{1212}\xi^2\eta & -D_{1111}\xi^4 - 4D_{1212}\xi^2\eta^2 - D_{2222}\eta^4 - 2D_{1122}\xi^2\eta^2 & 2F_{1221}\xi\eta^2 + F_{1111}\xi^3 + F_{2211}\xi\eta^2 & F_{1112}\xi^2\eta + 2F_{1222}\xi^2\eta + F_{2212}\eta^3 \\ -E_{1111}\xi^2 - E_{1221}\eta^2 & -E_{2211}\xi\eta - E_{1221}\xi\eta & 2F_{1221}\xi\eta^2 + F_{1111}\xi^3 + F_{2211}\xi\eta^2 & -G_{1111}\xi^2 - G_{2121}\eta^2 - H_{1212} & -G_{1112}\xi\eta - G_{2122}\xi\eta \\ -E_{1112}\xi\eta - E_{1222}\xi\eta & -E_{1222}\xi^2 - E_{2212}\eta^2 & F_{1112}\xi^2\eta + 2F_{1222}\xi^2\eta + F_{2212}\eta^3 & -G_{1112}\xi\eta - G_{2122}\xi\eta & -G_{2222}\xi^2 - G_{1212}\eta^2 - H_{2323} \end{bmatrix} \tag{A.3}$$

$$K_2 = \begin{bmatrix} -2A_{1112}\xi\eta & -A_{2212}\eta^2 - A_{1112}\xi^2 & -B_{2212}\eta^3 - 3B_{1112}\xi^2\eta & -E_{1211}\xi\eta - E_{1121}\xi\eta & -E_{1122}\xi^2 - E_{1212}\eta^2 \\ -A_{2212}\eta^2 - A_{1112}\xi^2 & -2A_{2212}\xi\eta & -B_{1112}\xi^3 - 3B_{2212}\xi\eta^2 & -E_{2221}\eta^2 - E_{1211}\xi^2 & -E_{1212}\xi\eta - E_{2222}\xi\eta \\ 3B_{1112}\xi^2\eta + B_{2212}\eta^3 & 3B_{2212}\xi\eta^2 + B_{1112}\xi^3 & 4D_{1112}\xi^3\eta + 4D_{2212}\xi\eta^3 & F_{2221}\eta^3 + 2F_{1211}\xi^2\eta + F_{1121}\xi^2\eta & F_{1122}\xi^3 + F_{2222}\xi\eta^2 + 2F_{1212}\xi\eta^2 \\ -E_{1211}\xi\eta - E_{1121}\xi\eta & -E_{2221}\eta^2 - E_{1211}\xi^2 & -2F_{1211}\xi^2\eta - F_{2221}\eta^3 - F_{1121}\xi^2\eta & -2G_{1121}\xi\eta & -G_{1221}\eta^2 - H_{1213} - G_{1122}\xi^2 \\ -E_{1122}\xi^2 - E_{1212}\eta^2 & -E_{1212}\xi\eta - E_{2222}\xi\eta & -2F_{1212}\xi\eta^2 - F_{1122}\xi^3 - F_{2222}\xi\eta^2 & -G_{1221}\eta^2 - H_{1213} - G_{1122}\xi^2 & -2G_{1222}\xi\eta \end{bmatrix} \tag{A.4}$$

$$K_3 = \begin{bmatrix} -2A_{1112}\xi\eta & -A_{2212}\eta^2 - A_{1112}\xi^2 & 3B_{1112}\xi^2\eta + B_{2212}\eta^3 & -E_{1211}\xi\eta - E_{1121}\xi\eta & -E_{1122}\xi^2 - E_{1212}\eta^2 \\ -A_{2212}\eta^2 - A_{1112}\xi^2 & -2A_{2212}\xi\eta & 3B_{2212}\xi\eta^2 + B_{1112}\xi^3 & -E_{2221}\eta^2 - E_{1211}\xi^2 & -E_{1212}\xi\eta - E_{2222}\xi\eta \\ -B_{2212}\eta^3 - 3B_{1112}\xi^2\eta & -B_{1112}\xi^3 - 3B_{2212}\xi\eta^2 & 4D_{1112}\xi^3\eta + 4D_{2212}\xi\eta^3 & -2F_{1211}\xi^2\eta - F_{2221}\eta^3 - F_{1121}\xi^2\eta & -2F_{1212}\xi\eta^2 - F_{1122}\xi^3 - F_{2222}\xi\eta^2 \\ -E_{1211}\xi\eta - E_{1121}\xi\eta & -E_{2221}\eta^2 - E_{1211}\xi^2 & F_{2221}\eta^3 + 2F_{1211}\xi^2\eta + F_{1121}\xi^2\eta & -2G_{1121}\xi\eta & -G_{1221}\eta^2 - H_{1213} - G_{1122}\xi^2 \\ -E_{1122}\xi^2 - E_{1212}\eta^2 & -E_{1212}\xi\eta - E_{2222}\xi\eta & F_{1122}\xi^3 + F_{2222}\xi\eta^2 + 2F_{1212}\xi\eta^2 & -G_{1221}\eta^2 - H_{1213} - G_{1122}\xi^2 & -2G_{1222}\xi\eta \end{bmatrix} \tag{A.5}$$

$$K_4 = \begin{bmatrix} -A_{1212}\eta^2 - A_{1111}\xi^2 & -A_{1122}\xi\eta - A_{1212}\xi\eta & -2B_{1212}\xi\eta^2 - B_{1111}\xi^3 - B_{1122}\xi\eta^2 & -E_{1111}\xi^2 - E_{1221}\eta^2 & -E_{1112}\xi\eta - E_{1222}\xi\eta \\ -A_{1122}\xi\eta - A_{1212}\xi\eta & -A_{2222}\eta^2 - A_{1212}\xi^2 & -B_{1122}\xi^2\eta - B_{2222}\eta^3 - 2B_{1212}\xi^2\eta & -E_{2211}\xi\eta - E_{1221}\xi\eta & -E_{1222}\xi^2 - E_{2212}\eta^2 \\ -2B_{1212}\xi\eta^2 - B_{1111}\xi^3 - B_{1122}\xi\eta^2 & -B_{1122}\xi^2\eta - B_{2222}\eta^3 - 2B_{1212}\xi^2\eta & -D_{1111}\xi^4 - 4D_{1212}\xi^2\eta^2 - D_{2222}\eta^4 - 2D_{1122}\xi^2\eta^2 & -F_{1111}\xi^3 - F_{2211}\xi\eta^2 - 2F_{1221}\xi\eta^2 & -F_{1112}\xi^2\eta - F_{2212}\eta^3 - 2F_{1222}\xi^2\eta \\ -E_{1111}\xi^2 - E_{1221}\eta^2 & -E_{2211}\xi\eta - E_{1221}\xi\eta & -F_{1111}\xi^3 - F_{2211}\xi\eta^2 - 2F_{1221}\xi\eta^2 & -G_{1111}\xi^2 - G_{2121}\eta^2 - H_{1212} & -G_{1112}\xi\eta - G_{2122}\xi\eta \\ -E_{1112}\xi\eta - E_{1222}\xi\eta & -E_{1222}\xi^2 - E_{2212}\eta^2 & -F_{1112}\xi^2\eta - F_{2212}\eta^3 - 2F_{1222}\xi^2\eta & -G_{1112}\xi\eta - G_{2122}\xi\eta & -G_{2222}\xi^2 - G_{1212}\eta^2 - H_{2323} \end{bmatrix} \tag{A.6}$$

$$M_1 = \begin{bmatrix} R & 0 & -S\xi & U_{11} & 0 \\ 0 & R & -S\eta & 0 & U_{22} \\ -S\xi & -S\eta & R + T\xi^2 + T\eta^2 & -V_{11}\xi & -V_{22}\eta \\ U_{11} & 0 & -V_{11}\xi & W_{11} & 0 \\ 0 & U_{22} & -V_{22}\eta & 0 & W_{22} \end{bmatrix} \qquad M_2 = \begin{bmatrix} 0 & 0 & 0 & 0 & U_{12} \\ 0 & 0 & 0 & U_{21} & 0 \\ 0 & 0 & 0 & -V_{21}\eta & -V_{12}\xi \\ 0 & U_{21} & V_{21}\eta & 0 & W_{12} \\ U_{12} & 0 & V_{12}\xi & W_{21} & 0 \end{bmatrix} \tag{A.7}$$

$$M_3 = \begin{bmatrix} 0 & 0 & 0 & 0 & U_{12} \\ 0 & 0 & 0 & U_{21} & 0 \\ 0 & 0 & 0 & V_{21}\eta & V_{12}\xi \\ 0 & U_{21} & -V_{21}\eta & 0 & W_{12} \\ U_{12} & 0 & -V_{12}\xi & W_{21} & 0 \end{bmatrix} \qquad M_4 = \begin{bmatrix} R & 0 & S\xi & U_{11} & 0 \\ 0 & R & S\eta & 0 & U_{22} \\ S\xi & S\eta & R + T(\xi^2 + \eta^2) & V_{11}\xi & V_{22}\eta \\ U_{11} & 0 & V_{11}\xi & W_{11} & 0 \\ 0 & U_{22} & V_{22}\eta & 0 & W_{22} \end{bmatrix} \tag{A.8}$$